Nonautonomous matter-wave solitons near the Feshbach resonance

V. N. Serkin,[1] Akira Hasegawa,[2] and T. L. Belyaeva[1]

[1]*Benemerita Universidad Autonoma de Puebla, Instituto de Ciencias, A.P. 502, 72001 Puebla, Mexico*

[2]*Soliton Communications, #403, 19-1 Awataguchi Sanjobocho, Higashiyama-ku, Kyoto 605-0035, Japan*

(Received 2 September 2008; revised manuscript received 23 November 2009; published 17 February 2010)

By means of analytical and numerical methods, we reveal the main features of nonautonomous matter-wave solitons near the Feshbach resonance in a one-dimensional Bose-Einstein condensate confined by a harmonic potential with a varying-in-time longitudinal trapping frequency. Based on the generalized nonautonomous Gross-Pitaevskii model, we show that solitons in nonautonomous physical systems exist only under certain conditions so that varying-in-time nonlinearity and confining harmonic potential cannot be chosen independently; they satisfy the exact integrability scenarios and complement each other. We focus on the most physically important examples where the applied magnetic field is either a linearly or a periodically varying-in-time function. In the case of periodically varying scattering length, variations of confining harmonic potential are found to be sign-reversible (periodic attractive and repulsive) to support the soliton-management regime. We investigate the losses of validity of one-dimensional (1D) approximation in the cases when, by the joint action of varying-in-time nonlinearity and confining potential, the atom cloud can be compressed from an initially elongated quasi-1D cigar-shaped geometry to a final ball-shaped three-dimensional geometry and the induced soliton collapse may occur.

DOI: 10.1103/PhysRevA.81.023610 PACS number(s): 03.75.Lm, 03.75.Kk, 05.45.Yv, 34.50.−s

I. INTRODUCTION

The discovery of Bose-Einstein condensate (BEC) in trapped clouds of ultracold alkali-metal atoms opened unique possibilities to investigate the wave nature of matter [1–11]. This has been shown in the elegant BEC experiments that discover, among other things, dark and bright matter-wave solitons [6–11].

Being a product of the high-speed computer revolution of the 20th century [12], the soliton is a subject of much current interest in nonlinear science. Zabusky and Kruskal introduced for the first time the soliton concept to characterize nonlinear solitary waves that do not disperse and preserve their identity during propagation and after a collision. The Greek ending "on" is generally used to describe elementary particles and this word was introduced to emphasize the most remarkable feature of these solitary waves. This means that the energy can propagate in the localized form and that the solitary waves emerge from the interaction completely preserved in form and speed with only a phase shift. Because of these defining features, the classical soliton is being considered as the ideal natural data bit. The optical soliton in fibers presents a beautiful example in which an abstract mathematical concept has produced a large impact on the real world of high technologies [13,14].

The classical soliton concept was developed for nonlinear and dispersive systems that have been autonomous; namely, time has only played the role of the independent variable and has not appeared explicitly in the nonlinear evolution equation. A not uncommon situation is one in which a system is subjected to some form of external time-dependent force. Such situations could include repeated stress testing of a soliton in nonuniform media with time-dependent density gradients; these situations are typical for experiments with temporal and/or spatial optical solitons, soliton lasers, ultrafast soliton switches, and logic gates. The formation of matter-wave solitons in BEC by magnetically tuned the interatomic interaction near a Feshbach resonance provides a good example of nonautonomous nonlinear system [8–10].

Historically, the study of soliton propagation through density gradients began with the pioneering work of Tappert and Zabusky [15]. As early as 1976, Chen and Liu [16] substantially extended the concept of classical solitons to the accelerated motion of a soliton in a linearly inhomogeneous plasma. It was discovered that for the nonlinear Schrödinger equation (NLSE) model with a linear external potential $V_{\text{ext}}(x,t) = \alpha_0 x$ the inverse scattering transform (IST) method [17] can be generalized by allowing the time-varying eigenvalue (TVE), and as a consequence of this, the solitons with time-varying velocities (but with time-invariant amplitudes) have been predicted [16]. At the same time, Calogero and Degaspieris [18] introduced the general class of soliton solutions for the nonautonomous Korteweg–de Vries (KdV) models with varying nonlinearity and dispersion. It was shown that the basic property of solitons, to interact elastically, was also preserved, but a novel phenomenon was demonstrated, namely, the fact that each soliton generally moves with variable speed as a particle acted on by an external force rather than as a free particle [18]. In particular, to appreciate the significance of this analogy, Calogero and Degaspieris introduced the terms boomeron and trappon instead of classical KdV solitons [18]. More recently, different aspects of soliton dynamics described by the nonautonomous NLSE models were investigated in Refs. [19,20]. The "ideal" solitonlike interaction scenarios among solitons have been studied in [19,20] in the framework of the generalized nonautonomous NLSE models with varying dispersion, nonlinearity, and dissipation or gain. Exact soliton solutions for the nonautonomous nonlinear Schrödinger equation models with linear and harmonic oscillator potentials substantially extend the concept of classical solitons and generalize it to the plethora of nonautonomous solitons that interact elastically and generally move with varying amplitudes, speeds, and spectra adapted both to the external potentials and to the dispersion and nonlinearity variations.

In this work, we clarify our algorithm based on the Lax pair generalization [20] and reveal generic properties of nonautonomous matter-wave solitons. We consider the generalized nonautonomous NLSE models with varying nonlinearities from the point of view of their exact integrability for both confining and expulsive external potentials. We emphasize that the main goal of the article is twofold. First, we construct the exactly integrable models for the Feshbach resonance soliton management and investigate their main features by analyzing the exact analytical solutions. Second, by means of direct computer experiments, we demonstrate the stability of matter-wave nonautonomous solitons and investigate the validity of one-dimensional (1D) theory.

Our theory establishes an important interconnection between the varying-in-time nonlinearity and confining potential. The exact analytical solutions and numerical simulations reveal many specific features of nonautonomous solitons corresponding to the different experimental conditions. To date, bright matter-wave solitons and trains of bright solitons have been studied in experiments with Bosonic lithium having attractive interactions [8,9]. The experimental realization was possible by tuning the scattering length with a Feshbach resonance, first producing a condensate with repulsive interactions, loading it into a 1D geometry, and then switching the interaction to attractive by a change in the magnetic offset field. Matter-wave dark solitons have been realized in most experiments by using the so-called "phase imprinting" method [5–7]. However, much less attention has been paid to studying the behavior of solitons in BECs exhibiting both varying-in-time nonlinearity and appropriately varying-in-time trapping potential. Up to now, no attempts had been made in experiments to relate these two different management scenarios and to find nontrivial laws of soliton adaptation in external potentials when varying-in-time nonlinearity and confining potential complement each other.

A subtle interplay between nonlinear management by means of the Feshbach resonance on the one hand and varying-in-time harmonic oscillator potential on the other hand can result in a rich variety of matter-wave solitons with several interesting properties. To test the validity of our predictions, the experimental arrangement should be inspected to be as close as possible to the optimal map of parameters at which the problem proves to be exactly integrable. The exact analytical solutions and numerical experiments reveal many specific features of nonautonomous solitons near the Feshbach resonance. We propose the experimentally accessible methods to generate the BEC solitons and demonstrate that variations of magnetically tuned scattering length must be consistent with variations of the confining potential. It is found, in particular, that near a Feshbach resonance the matter-wave soliton can be stabilized even without an axial trapping potential. In the case of periodically varying nonlinearity, variations of the external harmonic potential are found to be periodically sign-reversible (expulsive or attractive) in time. We demonstrate the advantages and limitations of our 1D approximation. The Gross-Pitaevskii (GP) wave equation, as is well known, predicts the catastrophic collapse of self-focusing beams in two-dimensional (2D) and three-dimansional (3D) space configurations [2–4]. By means of direct computer experiments, we study the losses of validity of 1D theory leading to matter-wave soliton collapse induced by 1D-to-3D transformations of trapping potentials. Based on computer simulations, we find that 1D nonautonomous matter-wave soliton exists if varying-in-time scattering length $a_s(t)$ and 1D condensate density $n_{1D}(t)$ satisfy the following "empirical" condition: $|a_s(t)|n_{1D}(t) \leqslant 0.1$.

To avoid confusion, we stress that exclusively the integrable models are being considered and investigated in this article. Nonintegrable models for the Feshbach resonance nonlinear management of matter waves are summarized in the recently published book [4].

The article is organized as follows. In Sec. II we discuss the statement of the problem and consider certain of the remarkable opportunities for strong nonlinear soliton management that are specific to only the Feshbach resonance. In Sec. III we consider the generalized nonautonomous GP models from the point of view of their exact integrability by the IST method and obtain the general solutions for these models. In Sec. IV we study the main features of nonautonomous matter-wave solitons near the Feshbach resonance with continuously tuned scattering length. We consider the two most physically important examples when the applied magnetic field is varying in time linearly and periodically. The nonautonomous soliton management concept presented in this article is strictly valid for the limiting case of 1D condensate. Obviously, this model has explicit and implicit limitations on its applicability. Some of the advantages and limitations of 1D soliton management concept will be demonstrated in Sec. V through direct 3D computer simulations. Finally, Sec. VI contains the conclusions drawn from our study and an outlook for future work.

II. STRONG VARIATIONS OF NONLINEARITY NEAR THE FESHBACH RESONANCE

It is a commonly accepted fact that the evolution of the condensate wave function $\Psi(\mathbf{r}, t)$ may be very accurately described by the 3D model well known in low-temperature and solid-state physics named, after its authors, the Gross-Pitaevskii (3D GP) model [2–4,21]:

$$i\hbar\frac{\partial}{\partial t}\Psi(\mathbf{r}, t)=\left[-\frac{\hbar^2\nabla^2}{2m}+G_0\ |\Psi(\mathbf{r}, t)|^2+V_{\text{ext}}(\mathbf{r}, t)\right]\Psi(\mathbf{r}, t), \tag{1}$$

the time-independent version of which,

$$\left[-\frac{\hbar^2\nabla^2}{2m}+G_0\ |\Phi(\mathbf{r})|^2+V_{\text{ext}}(\mathbf{r})\right]\Phi(\mathbf{r})=\mu\Phi(\mathbf{r}), \tag{2}$$

is derived by means of the ansatz

$$\Psi(\mathbf{r}, t)=\Phi(\mathbf{r})\exp(-i\mu t/\hbar), \tag{3}$$

where we use the standard notation for the chemical potential μ and the time-independent nonlinear parameter G_0,

$$G_0=\frac{4\pi\hbar^2 a_s}{m}=\text{const}. \tag{4}$$

In these equations $\mathbf{r}=(x, y, z)$ is the displacement from the trap $V_{\text{ext}}(\mathbf{r})$ center and m refers to the mass of the atom. The condensate wave function is normalized to the total number of

atoms in BEC,

$$\int |\Psi(\mathbf{r}, t)|^2 \, d^3\mathbf{r} = N = \text{const}, \tag{5}$$

and the density of atoms is given by

$$n_{3D}(\mathbf{r}) = |\Psi(\mathbf{r}, t)|^2 . \tag{6}$$

From the physical point of view, the dynamics of condensate can be treated as a substantially nonlinear process, which is completely similar to the formation of the Bose condensate of photons in a laser [22]. In the absence of an external potential, the GP equation is ordinarily considered to be like the NLSE, which is well studied in the theory of the self-focusing and generation of temporal and spatial optical solitons [23–29].

The nonlinearity in BEC arises from the density-dependent interactions between atoms proportional to the s-wave scattering length a_s [1–4,21]. These interactions add significant new physics to the coherent matter wave itself and give rise to many novel phenomena in analogy to general nonlinear wave effects [2–4]. Matter-wave solitons are formed due to the balance of the dispersion and nonlinear compression. In a Bose-Einstein condensate this balance occurs between the nonlinear mean-field interaction and quantum pressure and can be classified according to the sign of the s-wave scattering length, a_s, determining whether the interparticle interaction is attractive (negative a_s) or repulsive (positive a_s) and leading, respectively, to the formation of bright or dark solitons. The magnetic-field dependence of the scattering length a_s has a resonance structure near the so-called Feshbach resonances [30–36], that provides remarkable opportunities for the study of matter-wave physics with a very strong, very weak, positive, negative, or even time-dependent interaction strength, all within a single experiment [30–36].

In the general case, the strength of the nonlinearity $G_{3D}(t)$ is defined in terms of the time-dependent s-wave scattering length $a_s(t)$,

$$G_{3D}(t) = \frac{4\pi\hbar^2 a_s(t)}{m}. \tag{7}$$

As follows from experiments [30–36], the resonance in the s-wave scattering length $a(B)$ shows a dispersive form as a function of the applied magnetic field,

$$\frac{a_s(B)}{a_{bg}} = 1 + \frac{\Delta_0/B_0}{1 - B(t)/B_0}. \tag{8}$$

This kind of energy-dependent enhancement of interparticle collision cross sections arises because of the existence of a metastable state [2–4]. In the empirically derived expression Eq. (8), B_0 is the resonant value of the magnetic field, a_{bg} is the value of scattering length far from resonance, and parameter Δ_0 represents the resonance width in units of the Bohr radius $a_0 = 0.0529$ nm. Feshbach resonances have been reported in ^{85}Rb at 164 G [33], in ^{23}Na at 853 and 907 G [32], and in ^{7}Li at 725 G [8]. ^{133}Cs offers further flexibility because of a unique combination of low-field Feshbach resonances [36]: one broad resonance allows for precise tuning of the scattering length from a large negative value at zero field to large positive values at higher fields going through zero at 17 G, whereas several narrow resonances (with the most prominent one at 48 G) enable very precise control [36].

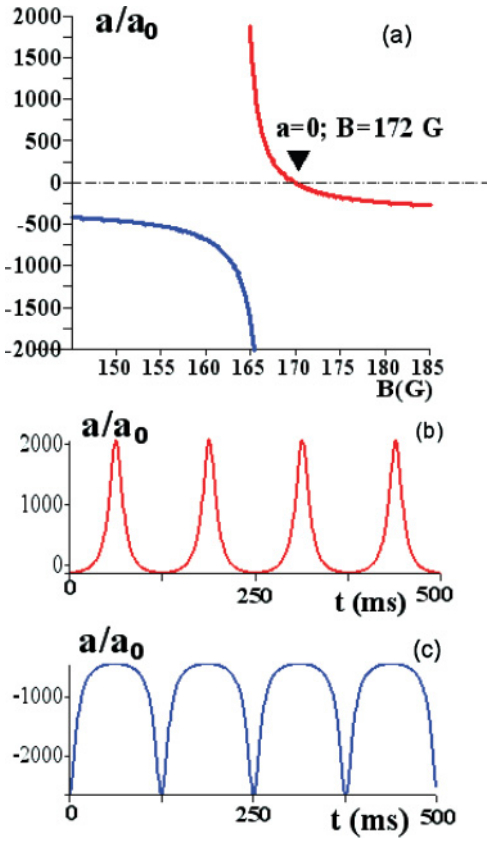

FIG. 1. (Color online) Feshbach resonance management. (a) The resonance structure in the magnetic-field-dependence of the scattering length a_s. (b) Variations in time of the scattering length in the case of periodical sweeping of the magnetic field across the point 172 G. (c) Variations in time of the scattering length in the case of periodical sweeping of the magnetic field through the point 156 G.

Let us consider the Feshbach resonance nonlinear management problem in more detail. As an example, and without the loss of generality, we consider the main Feshbach resonance characteristics obtained in experiments with ^{85}Rb [33]. These experiments demonstrate that the self-interaction energy of the ^{85}Rb Bose-Einstein condensate can be magnetically tuned in accordance with the dispersive form given by empirical relation Eq. (8), where $a_{bg} = -295a_0$, $\Delta_0 = 8$ G, and $B_0 = 164$ G.

Calculated magnetic-field dependence of scattering length (corresponding resonance value $B_0 = 164$ G and width of resonance $\Delta_0 = 8$ G) is shown in Fig. 1(a). The scattering length becomes zero at 172 G. This figure indicates that the nonlinear term given by Eq. (4) can be continuously tuned if the magnetic field will vary in time. In particular, the variations of the scattering length by almost two orders of magnitude can be obtained during 500 ms by linearly tuning the magnitude of the magnetic field $B = B(t = 0) + \gamma t - B_0$ with the speed of the field ramp $\gamma = dB/dt = 0.08$ G/ms in the range $B = (145–185)$ G. The scattering length as a function of time has the same form as represented in Fig. 1(a) with the only difference being that the point at which 185 G corresponds to the total time interval 500 ms and the peak of the resonance 164 G now corresponds to 250 ms.

The variation of the scattering length near the Feshbach resonance has been used in experiments by Cornish *et al.* [34] to magnetically tune the condensate self-interaction energy over a wide range, extending from strong repulsive to large attractive interactions. Cornish *et al.* [34] applied a linear ramp to sweep the magnetic field across the resonance. By applying a linear ramp to the magnetic field, they varied the magnitude of the scattering length in the condensate by almost three orders of magnitude. Cornish *et al.* [34] especially emphasized that the duration of this ramp (500 ms) was chosen to be sufficiently long to ensure that the condensate responded adiabatically.

There is still much room for improvement in employing the Feshbach resonance management technique. One important possibility can be demonstrated. Let us consider, for example, the periodical sweeping of the magnetic field near the Feshbach resonance. Figure 1(b) shows the time dependence of scattering length (in units of the Bohr radius) corresponding to the magnetic field variations $B(t) = B(t = 0) + \beta \cos(\varpi t) - B_0$ around the zero scattering length point $B(t = 0) = 172$ G with the amplitude of the field modulation $\beta = 7$ G and the frequency $\varpi = 16\pi$ rad/s ($T = 2\pi/\varpi = 125$ ms). The sweeping of the magnetic field through the zero point $a = 0$ at $B = 172$ G toward the Feshbach resonance $B = 164$ G is responsible for the scattering length increasing. For comparison, Fig. 1(c) illustrates how we are able to easily change the scattering length dynamics by moving in the opposite direction and sweeping of the magnetic field across the point $B(t = 0) = 156$ G where the scattering length becomes negative.

III. EXACTLY INTEGRABLE MODELS FOR MATTER-WAVE SOLITONS NEAR THE FESHBACH RESONANCES IN CONFINING POTENTIALS

The intrinsic similarities between the mean-field GP model and the NLSE model imply the existence of common fundamental nonlinear phenomena, independent of the physical origin of the nonlinearity. Equation (1) is known for a large class of physical systems, and without confining potential this equation is known as the famous nonlinear Schrödinger equation. In this sense, matter-wave solitons in one dimension are similar to optical solitons in fibers [23–29] and, therefore, the parallelism with the fiber-soliton management concept could be brought into active use for matter waves as well (see, for example, the review of optical soliton dispersion management principles in [14,29] and references therein).

How can we determine whether a given nonlinear evolution equation is integrable? An ingenious method for answering this question was discovered by Gardner, Green, Kruskal, and Miura (GGKM) [17]. Following this work, Lax [37] formulated a general principle for associating nonlinear evolution equations with linear operators so that the eigenvalues of the linear operator are integrals of the nonlinear equation. Lax developed the IST method based on an abstract formulation of evolution equations and certain properties of operators in a Hilbert space, some of which are well known in the context of quantum mechanics [17]. Ablowitz, Kaup, Newell, and Segur (AKNS) [38] have found that many physically meaningful nonlinear models can be solved with the IST method.

In the traditional scheme of the IST method, the spectral parameter Λ of the auxiliary linear problem is assumed to be a time-independent constant $\Lambda_t' = 0$, and this fact plays a fundamental role in the development of analytical theory. Chen and Liu [16] were the first who showed theoretically that an inhomogeneous plasma still supports Langmuir solitons and multisolitons, which maintain their shapes and identities even after mutual collisions if and only if $\Lambda_t' = \text{const} = \alpha_0$. The NLSE model with linear x-dependent potential was directly integrated in their work [16] by applying the IST method.

Notice that the nonlinear evolution equations that arise in the approach of the variable spectral parameter, $\Lambda_t' \neq 0$, contain, as a rule, some coefficients explicitly dependent on time. In physics and mathematics, a differential equation is autonomous when it does not depend on time (does not depend on the independent variable). In contrast, differential equation is nonautonomous when it does depend on time (does depend on the independent variable). The classification of dynamic systems into autonomous and nonautonomous is often convenient and can correspond to different physical situations, in which, respectively, an external time-dependent driving force is present or absent. The mathematical treatment of a nonautonomous system of equations is considerably more complicated then the treatment of autonomous ones.

The IST method with variable spectral parameter makes it possible not only to construct the well-known models of nonlinear autonomous physical systems, but also to discover many novel integrable and physically significant nonlinear nonautonomous equations by extending the Zakharov-Shabat (ZS) [39] and AKNS [38] formalism and following the ideas of Chen and Liu [16], Calogero and Degasperis [18], and Gupta, Ray, Herrera, and Balakrishnan [40].

In the framework of the generalized IST method with the variable spectral parameter $\Lambda(t)$, a nonlinear integrable equation arises as a compatibility condition,

$$\widehat{\mathcal{F}}_t - \widehat{\mathcal{G}}_x + [\widehat{\mathcal{F}}, \widehat{\mathcal{G}}] = 0, \tag{9}$$

of a system of the eigenvalue linear matrix differential equations:

$$\psi_x = \widehat{\mathcal{F}}\psi(x,t), \quad \psi_t = \widehat{\mathcal{G}}\psi(x,t). \tag{10}$$

Here $\psi(x,t) = \{\psi_1, \psi_2\}^T$ is a two-component complex function, $\widehat{\mathcal{F}}$ and $\widehat{\mathcal{G}}$ are complex-valued (2×2) matrices,

$$\widehat{\mathcal{F}}(\Lambda) = \widehat{\mathcal{F}}\left\{\Lambda(t), Q(x,t), \frac{\partial Q}{\partial x}, \frac{\partial^2 Q}{\partial x^2}\right\}, \tag{11}$$

$$\widehat{\mathcal{G}}(\Lambda) = \widehat{\mathcal{G}}\left\{\Lambda(T), Q(x,t), \frac{\partial Q}{\partial x}, \frac{\partial^2 Q}{\partial x^2}\right\}, \tag{12}$$

depending on the time-varying spectral parameter $\Lambda(t) = \kappa(t) + i\eta(t)$. Following the general strategy based on the IST-TVE method discovered by Chen and Liu [16] and applying the moving-in-time focuses concept of the self-focusing theory to the fundamental IST-TVE formalism (see, e.g., [19], and references therein), we can construct the desired matrices $\widehat{\mathcal{F}}$ and $\widehat{\mathcal{G}}$ in the form

$$\widehat{\mathcal{F}} = -i\Lambda(t)\widehat{\sigma}_3 + \widehat{U}\widehat{\phi}, \tag{13}$$

$$\widehat{\mathcal{G}} = \begin{pmatrix} A & B \\ C & -A \end{pmatrix}, \tag{14}$$

$$\widehat{U} = \sqrt{\frac{\sigma}{1-\Phi(t)}} \begin{pmatrix} 0 & Q(x,t) \\ -Q^*(x,t) & 0 \end{pmatrix}, \tag{15}$$

$$\widehat{\phi} = \begin{pmatrix} \exp[-i\Phi_t(1-\Phi)^{-1}x^2/2] & 0 \\ 0 & \exp[i\Phi_t(1-\Phi)^{-1}x^2/2] \end{pmatrix}. \tag{16}$$

The desired AKNS elements [38,39] of the $\widehat{\mathcal{G}}$ matrix, $\widehat{\mathcal{G}} = \sum_{k=0}^{k=2} G_k \Lambda^k$, with

$$\Lambda_t = \alpha(t) + \Lambda(t)\frac{\Phi_t}{(1-\Phi)},$$

are represented by

$$\begin{aligned} A &= \frac{i}{2}\frac{\sigma}{1-\Phi}|Q|^2 - i\alpha(t)x - i\Lambda x\frac{\Phi_t}{(1-\Phi)} - i\Lambda^2, \\ B &= \sqrt{\frac{\sigma}{1-\Phi}}\left[\frac{1}{2}xQ\frac{\Phi_t}{(1-\Phi)} + \frac{i}{2}Q_x + \Lambda Q\right] \\ &\quad \times \exp\left[i\frac{\Phi_t x^2}{2(1-\Phi)}\right] \\ C &= -B^*. \end{aligned} \tag{17}$$

The Schrödinger equation is of the second order of x, which is why we have considered here terms not higher than the second order of Λ.

Equation (9) must be valid for all values of complex TVE $\Lambda(t) = \kappa(t) + i\eta(t)$

$$\begin{aligned} \Lambda(t) &= \kappa(t) + i\eta(t) \\ &= \frac{1-\Phi(0)}{1-\Phi(t)}\left[\Lambda(0) + \int_0^t \alpha(t')\frac{1-\Phi(t')}{1-\Phi(0)}dt'\right], \end{aligned} \tag{18}$$

where $\Lambda(0) = k_0 + i\eta_0$ is given by the initial conditions. The function $\Phi(t)$ is required to be a twice-differentiable and once-integrable, but otherwise arbitrary, function; there are no restrictions. We call it control function here and assume that $\Phi(t=0) = \Phi(0)$.

From the mathematical point of view, the main problem is to find a suitable transformation under which the symmetric form of the Lax equation is preserved. Alternatively, from the physical point of view, the more fundamental is the question whether the inhomogeneous media still support solitons with varying main parameters: variable time-space duration, amplitude, and phase. To find a such transformation, we introduce matrix

$$\widehat{\phi} = \begin{pmatrix} \exp[i\varphi(x,t)] & 0 \\ 0 & \exp[-i\varphi(x,t)] \end{pmatrix}, \tag{19}$$

where the function $\varphi(x,t)$ is defined by the parabolic phase profile $\varphi = \Theta(t)x^2/2$. The transformation (19) directly follows from the general Hamiltonian approach and the well-known time-space analogy in the theory of self-focusing of laser beams in nonlinear optics [24–27]. The oscillating periodically contracted and expanded laser beam in self-focusing nonlinear Kerr-like media exists if and only if the radius of curvature of its wave front is an oscillating function of the propagation distance. More exactly, if we compare the expression for the phase profile given by Eq. (19) with a well-known formula for the ideal lens, $\varphi = r^2/2f$, we can conclude that the transformation law (19) can be considered as the transformation of the soliton phase by the nonlinear self-focusing lens with a time-dependent focus length $f = f(t)$.

The phase evolution of the condensate wave function can be studied in a well-defined and controlled way by means of interferometric methods during expansion as well as in a matter waveguide [41]. After release from the trap, the mean-field energy is converted to kinetic energy, which for an initial harmonic trapping potential leads to a quadratic phase profile. The results of the experimental and theoretical studies presented in Ref. [41] justify the phase transformation law given by Eq. (19).

The nonisospectral generalization for the IST method given by Eqs. (12)–(18) leads to the following exactly integrable nonautonomous NLSE model with parabolic time-dependent confining potential and linear (also time-dependent) potential:

$$\begin{aligned} &\left[i\frac{\partial}{\partial t} + \frac{1}{2}\frac{\partial^2}{\partial x^2} + \frac{\sigma}{1-\Phi(t)}|Q|^2\right]Q \\ &\quad = \left[2\alpha(t)x + \frac{1}{2}\frac{1}{1-\Phi(t)}\frac{\partial^2\Phi(t)}{\partial t^2}x^2\right]Q, \end{aligned} \tag{20}$$

where parameter $\sigma = \pm 1$ is introduced to separate bright- and dark-soliton solutions for the nonautonomous model given by Eq. (20).

When this result is compared with generalized nonautonomous GP equation,

$$i\frac{\partial Q}{\partial t} + \frac{1}{2}\frac{\partial^2 Q}{\partial x^2} + \sigma R(t)|Q|^2 Q - 2\alpha(t)xQ - \frac{1}{2}\Omega^2(t)x^2 Q = 0, \tag{21}$$

the exact integrability of the generalized GP model, Eq. (21), is immediately apparent if the time dependence of nonlinearity and variations of the confining potential satisfy the exact integrability scenario:

$$R(t) = \frac{1}{1-\Phi(t)}, \tag{22}$$

$$V(x,t) = \frac{1}{2}\Omega^2(t)\,x^2 = \frac{1}{2[1-\Phi(t)]}\frac{\partial^2\Phi(t)}{\partial t^2}x^2. \tag{23}$$

That is why solitons in nonautonomous physical systems exist only under certain conditions and varying-in-time nonlinearity and confining harmonic potential cannot be chosen independently; they satisfy the exact integrability scenarios and complement each other. From the physical point of view, Eq. (23) can be considered as the law of soliton adaptation to the external potential. It is precisely this soliton-adaptation mechanism that is of prime physical interest. Here, we clarify some examples in order to gain a better understanding into this physical mechanism, which can be considered as the interplay between nontrivial time-dependence of parabolic soliton phase and external time-dependent parabolic potential. We stress that this nontrivial time-space-dependent phase profile of nonautonomous soliton [see Eqs. (14) and (19)] depends on the management function $\Phi(t)$ and this profile does not exist for canonical NLSE soliton when $\Phi(t) = 0$ and $R(t) = 1$.

In this article, our investigations are focused on the main features of bright solitons near the Feshbach resonance. Dynamics of dark solitons will be considered in the separate publication.

Application of the auto-Bäcklund transformation [42] and the recurrent relation

$$Q_n(x,t) = -Q_{n-1}(x,t) - \frac{4\eta_n \mathbf{\Gamma}_{n-1}(x,t)}{1+|\mathbf{\Gamma}_{n-1}(x,t)|^2} \times [1-\Phi(t)] \exp\left[-i\frac{\Phi_t x^2}{2(1-\Phi)}\right], \tag{24}$$

which connects the $(n-1)$ and n-soliton solutions by means of the so-called pseudopotential $\mathbf{\Gamma}_{n-1}(x,t) = \psi_1(x,t)/\psi_2(x,t)$ for the $(n-1)$-soliton scattering functions $\psi(x,t) = (\psi_1\psi_2)^T$, leads us to the desired result. One-soliton $Q_1(x,t)$ and two-soliton $Q_2(x,t)$ solutions are represented by the following analytic expressions:

$$Q_1(x,t) = \frac{2\eta_{01}\,[1-\Phi(0)]}{\sqrt{(1-\Phi(t))}}\mathrm{sech}\,[\xi_1(x,t)] \times \exp\left[-i\frac{\Phi_t\, x^2}{2(1-\Phi)} - i\,\chi_1(x,t)\right], \tag{25}$$

$$Q_2(x,t) = 4\sqrt{(1-\Phi(t)}\frac{\mathcal{N}(x,t)}{\mathcal{D}(x,t)}\exp\left[-i\frac{\Phi_t x^2}{2(1-\Phi)}\right]. \tag{26}$$

In Eq. (26) the numerator is given by

$$\begin{aligned}\mathcal{N} = {}& \eta_1\cosh\xi_2\exp(-i\,\chi_1) \\ & \times\left[(\kappa_2-\kappa_1)^2 + i\,\eta_2(\kappa_2-\kappa_1)\tanh\xi_2 + \eta_1^2 - \eta_2^2\right] \\ & + \eta_2\cosh\xi_1\exp(-i\,\chi_2)\times\left[(\kappa_2-\kappa_1)^2\right. \\ & \left. - 2i\,\eta_1(\kappa_2-\kappa_1)\tanh\xi_1 - \eta_1^2+\eta_2^2\right],\end{aligned} \tag{27}$$

and the denominator is represented by

$$\begin{aligned}\mathcal{D} = {}& \cosh(\xi_1+\xi_2)[(\kappa_2-\kappa_1)^2+(\eta_1-\eta_2)^2] \\ & + \cosh(\xi_1-\xi_2)[(\kappa_2-\kappa_1)^2+(\eta_1+\eta_2)^2] \\ & - 4\eta_1\eta_2\cos(\chi_2-\chi_1),\end{aligned} \tag{28}$$

where

$$\begin{aligned}\xi_i(x,t) = {}& 2\eta_{0i}x\frac{1-\Phi(0)}{1-\Phi(t)} \\ & + 4\eta_{0i}\kappa_{0i}\,[1-\Phi(0)]^2\int_0^t\frac{d\tau}{[1-\Phi(\tau)]^2} \\ & + 4\eta_{0i}\,[1-\Phi(0)]\int_0^t\frac{d\tau}{[1-\Phi(\tau)]^2}\mathcal{K}(\tau),\end{aligned} \tag{29}$$

$$\begin{aligned}\chi_i(x,t) = {}& 2\kappa_{0i}x\frac{1-\Phi(0)}{1-\Phi(t)} + \frac{2x}{1-\Phi(t)}\mathcal{K}(t) \\ & + 2\left(\kappa_{0i}^2-\eta_{0i}^2\right)[1-\Phi(0)]^2\int_0^t\frac{d\tau}{[1-\Phi(\tau)]^2} \\ & + 4\kappa_{0i}\,[1-\Phi(0)]\int_0^t\frac{\mathcal{K}(\tau)d\tau}{[1-\Phi(\tau)]^2} \\ & + 2\int_0^t\left[\frac{\mathcal{K}(\tau)}{1-\Phi(\tau)}\right]^2 d\tau,\end{aligned} \tag{30}$$

$$\mathcal{K}(t) = \int_0^t \alpha(\tau')[1-\Phi(\tau')]d\tau', \tag{31}$$

$$\eta(t) = \frac{1-\Phi(0)}{1-\Phi(t)}\eta_{0i}, \quad \kappa(t) = \frac{1-\Phi(0)}{1-\Phi(t)}\kappa_{0i} + \frac{\mathcal{K}(t)}{1-\Phi(t)}, \tag{32}$$

and the initial velocity and amplitude of the ith soliton ($i=1,2$) are given by κ_{0i} and η_{0i}, respectively.

Equation (26) describes two-soliton bound state at all times and all locations. We will look into some of its interesting features. Obviously, these soliton solutions reduce to that obtained earlier in the limit $R(t)=1$, and $\alpha(t) = \Phi(t) \equiv 0$ for canonical NLSE without external potentials [23–29].

IV. NONLINEAR DYNAMICS OF NONAUTONOMOUS MATTER-WAVE SOLITONS NEAR THE FESHBACH RESONANCE WITH CONTINUOUSLY TUNED SCATTERING LENGTH

Equations (20) and (8) have one feature in common, the resonance form in the nonlinearity. That is why, as follows from Eqs. (20)–(23), the matter-wave soliton-management concept must be consistent with variations of confining potential.

Let us rewrite Eq. (21) in the vicinity of a resonance by using the reduction $\partial^2\Phi/\partial t^2 = 0$, which denotes that the confining harmonic potential is vanishing. To suppose that confining harmonic potential is vanishing implies that the control function $\Phi(t)$ is defined as $\Phi(t) = C_0 t$ with the initial condition $\Phi(0)=0$. Because of this, the nonlinearity in Eq. (21) has the simple dispersive form $R(t) = R(0)/(1-C_0 t)$, which holds also for the scattering length $a_s(t)$ in the case of the linear tuning of the magnetic field $B = B(t=0) + \gamma t - B_0$ [see Sec. II and Eq. (8)]. Without loss of generality, we consider $R(t=0)=1$. In fact, as we discussed in Sec. II, the scattering length $a_s(t)$ can be continuously tuned by linearly increasing in time an external magnetic field near the Feshbach resonance. Thus, we can write the following nonautonomous GP equation:

$$i\frac{\partial Q}{\partial t} + \frac{1}{2}\frac{\partial^2 Q}{\partial x^2} + \frac{1}{1-C_0 t}|Q|^2 Q - 2\alpha(t)xQ = 0. \tag{33}$$

Hence, the nonlinear BEC dynamics in the vicinity of the Feshbach resonance (8) can be considered in the framework of the exactly integrable NLSE model Eq. (32) with the nonlinearity of dispersive form. One- and two-soliton solutions in the most general form are given by

$$Q_1(x,t) = \frac{2\eta_{01}}{\sqrt{(1-C_0 t)}}\mathrm{sech}\,[\xi(x,t)] \times \exp\left[-\frac{i}{2}\frac{C_0 x^2}{1-C_0 t} - i\,\chi(x,t)\right], \tag{34}$$

$$Q_2(x,t) = 4\sqrt{(1-C_0 t)}\frac{\mathcal{N}(x,t)}{\mathcal{D}(x,t)}\exp\left(-\frac{i}{2}\frac{C_0 x^2}{1-C_0 t}\right), \tag{35}$$

where the nominator $\mathcal{N}(x,t)$ is given by Eq. (27), the denominator $\mathcal{D}(x,t)$ is represented by Eq. (28) and

$$\xi(x,t) = \frac{2\eta_{0i}x + 4\eta_{0i}\kappa_{0i}t}{1 - C_0 t} + 4\eta_{0i}\int_0^t \frac{d\tau}{(1 - C_0\tau)^2}\mathcal{K}'(\tau), \tag{36}$$

$$\chi(x,t) = \frac{2\kappa_{0i}x + 2\left(\kappa_{0i}^2 - \eta_{0i}^2\right)t + 2\mathcal{K}'(t)x}{1 - C_0 t} + 4\kappa_{0i}\int_0^t \frac{\mathcal{K}'(\tau)d\tau}{(1 - C_0\tau)^2} + 2\int_0^t \left[\frac{\mathcal{K}'(\tau)}{(1 - C_0\tau)}\right]^2 d\tau, \tag{37}$$

with

$$\mathcal{K}'(\tau) = \int_0^\tau \alpha(\tau')(1 - C_0\tau')d\tau' \tag{38}$$

and

$$\eta(t) = \frac{\eta_{0i}}{1 - C_0 t}, \quad \kappa(t) = \frac{\kappa_{0i}}{1 - C_0 t} + \mathcal{K}'(t). \tag{39}$$

Let us now give the explicit formulas of the soliton solutions for the case where all the eigenvalues are purely imaginary. In the case $\alpha = 0$, the one-soliton solution for Eq. (33) is given by

$$Q(x,t) = \frac{2\eta_{01}}{\sqrt{(1 - C_0 t)}}\mathrm{sech}\left[\frac{2\eta_{01}x}{(1 - C_0 t)}\right] \times \exp\left[-\frac{i}{2}\frac{C_0 x^2}{1 - C_0 t} + i\frac{2\eta_{01}^2}{(1 - C_0 t)}t\right]. \tag{40}$$

This result shows that in the vicinity of the Feshbach resonance the soliton can be stabilized even without a trapping potential and, in addition, Eq. (40) indicates the possibility for the optimal compression of matter-wave solitons in BEC. In this optimal regime the total energy is contained in the soliton. In Fig. 2 we illustrate the matter-wave soliton compression dynamics near the resonance given by Eq. (40) with $C_0 = 0.01$. Direct computer experiment confirms the linear-in-time soliton compression scenario in full accordance with analytical expression (40).

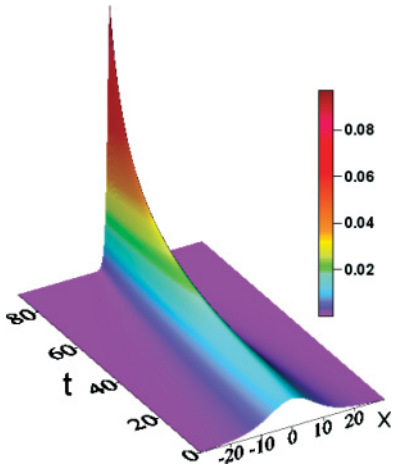

FIG. 2. (Color online) Self-compression of a nonautonomous matter-wave soliton near the Feshbach resonance calculated within the framework of the model [Eqs. (33), (40)] after choosing the soliton-management parameters $C_0 = 0.01$, $\alpha = 0$, and $\eta_0 = 0.05$.

The bound two-soliton solution for the case of the purely imaginary eigenvalues is represented by

$$Q_2(x,t) = 4\sqrt{(1 - C_0 t)}\frac{\mathcal{N}(x,t)}{\mathcal{D}(x,t)}\exp\left(-\frac{i}{2}\frac{C_0 x^2}{1 - C_0 t}\right), \tag{41}$$

where

$$\mathcal{N} = \left(\eta_1^2 - \eta_2^2\right)[\eta_1\cosh\xi_2\exp(-i\chi_1) - \eta_2\cosh\xi_1\exp(-i\chi_2)], \tag{42}$$

$$\mathcal{D} = \cosh(\xi_1 + \xi_2)(\eta_1 - \eta_2)^2 + \cosh(\xi_1 - \xi_2)(\eta_1 + \eta_2)^2 - 4\eta_1\eta_2\cos(\chi_2 - \chi_1), \tag{43}$$

and

$$\xi_i(x,t) = \frac{2\eta_{0i}x}{1 - C_0 t}, \tag{44}$$

$$\chi_i(x,t) = -\frac{2\eta_{0i}^2 t}{1 - C_0 t} + \chi_{0i}. \tag{45}$$

For the particular case of $\eta_{01} = 1/2$, $\eta_{02} = 3/2$, Eq. (41) transforms to

$$Q_2(x,t) = \frac{4}{\sqrt{(1 - C_0 t)}} \times \frac{\exp[it/2(1 - C_0 t) - \chi_{01}]}{\cosh 4x + 4\cosh 2x - 3\cos[4t/(1 - C_0 t) + \Delta\varphi]} \times \{\cosh 3x - 3\cosh x\exp[i4t/(1 - C_0 t) - \Delta\varphi]\}. \tag{46}$$

In the limit $R(t) = 1$ and $C_0 = 0$, this solution reduces to the well-known breather solution which was found by Satsuma and Yajima [43],

$$Q_2(x,t) = 4\frac{\cosh 3x + 3\cosh x\exp(4it)}{\cosh 4x + 4\cosh 2x + 3\cos 4t}\exp\left(\frac{it}{2}\right), \tag{47}$$

and has been observed in all pioneering experiments with optical solitons in fibers [23–29]. At $t = 0$, the breather takes the simple form $Q(x,t) = 2\mathrm{sech}(x)$. An interesting property of this breather solution is that its form oscillates with the so-called soliton period $T_{\mathrm{sol}} = \pi/2$ [23–29].

In the general case of nonautonomous system with time-dependent nonlinearity, the soliton period becomes dependent on time. Near the Feshbach resonance $R(t) = 1/(1 - C_0 t)$, the soliton period is given by

$$T_{\mathrm{sol}} = \frac{\pi(1 - C_0 t)^2}{\eta_{01}^2 - \eta_{02}^2}. \tag{48}$$

Typical behavior of nonautonomous breather is shown in Fig. 3 for $\eta_{01} = 0.25$, $\eta_{02} = 0.75$ and in Fig. 4 for $\eta_{01} = 0.4$, $\eta_{02} = 0.8$. Equation (48) can be obtained directly from

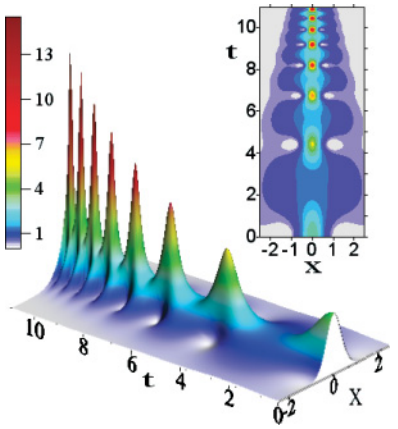

FIG. 3. (Color online) Matter-wave breather dynamics near the Feshbach resonance calculated within the framework of the model [Eq. (41)] after choosing the soliton-management parameters $C_0 = 0.07$, $\alpha = 0$, $\eta_{01} = 0.25$, and $\eta_{02} = 0.75$.

the general solution given by Eq. (46). We stress that the Satsuma and Yajima breather can be obtained from the general solution [Eq. (41)] if and only if the soliton phases are chosen properly, precisely when $\Delta\varphi = \pi$. The intensity profiles of the autonomous and nonautonomous breathers build up a complex landscape of peaks and valleys and reach their peaks at the points of the maximum (see Figs. 3 and 4).

The case of periodically varying magnetic field $B(t) = \beta\cos(\varpi t)$ can be regarded as a special case. In this case the spectral parameter $\Lambda(t)$ of the IST method is directly related to the magnetic field variations. Now the control function $\Phi(t)$ is given by $\Phi(t) = \beta\cos\varpi t$ and the parameter functions for varying-in-time nonlinearity $R(t)$ and confining potential $V(x,t)$ cannot be chosen independently; they satisfy

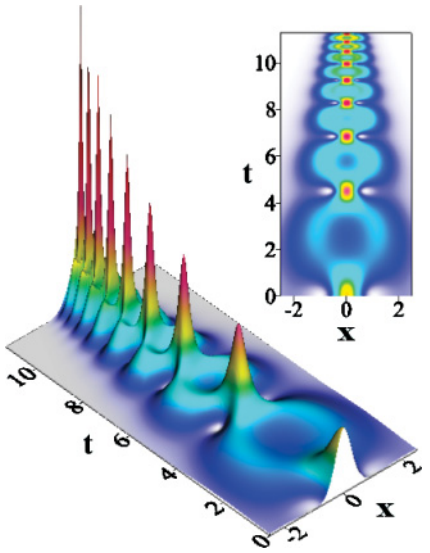

FIG. 4. (Color online) Two-nonautonomous-soliton-interaction scenario near the Feshbach resonance calculated within the framework of the model Eq. (41) after choosing the soliton-management parameters $C_0 = 0.07$, $\alpha = 0$, $\eta_{01} = 0.4$, and $\eta_{02} = 0.8$.

the following exact integrability conditions:

$$R(t) = \frac{1}{1+\beta\cos\varpi t}, \tag{49}$$

$$V(x,t) = \frac{1}{2}\Omega^2(t)x^2 = \frac{1}{2}\frac{\beta\varpi^2\cos\varpi t}{1+\beta\cos\varpi t}x^2. \tag{50}$$

Consequently, variations of confining harmonic potential are found to be sign-reversible (periodic attractive and repulsive) to support the stable nonlinear soliton-management scenario in this example. Exact soliton solutions for the case of periodically varying nonlinearity [Eq. (49)] are represented by formulas (25) and (29)–(32), where the substitution $\Phi(t) = \Phi_0\cos\varpi t$ is straightforward. Periodically varying in time the expulsive and/or attractive sign-reversible harmonic oscillator potential [Eq. (50)] makes it possible to generate nonautonomous matter-wave solitons with periodically varying characteristics (see Fig. 5).

Using the example of $\alpha = \alpha_0 = \text{const}$, one- and two-soliton solutions can be derived without difficulty. The result is given by the general solution [Eqs. (26)–(32)], where

$$\mathcal{K}(t) = \alpha_0 t\left(1 - \frac{C_0}{2}t\right), \tag{51}$$

$$\xi(x,t) = 2\eta_0(x + 2\kappa_0 t + \alpha_0 t^2)(1 - C_0 t)^{-1}, \tag{52}$$

$$\begin{aligned}\chi(x,t) = {} & \left[2\kappa_0 x + 2\alpha_0 x t + 2\left(\kappa_0^2 - \eta_0^2\right)t - \alpha_0 C_0 x t^2\right. \\ & \left. + 2\kappa_0\alpha_0 t^2\right](1 - C_0 t)^{-1} \\ & + \alpha_0^2\left(\frac{2}{3}t^3 - \frac{1}{6}C_0 t^4\right)(1 - C_0 t)^{-1}.\end{aligned} \tag{53}$$

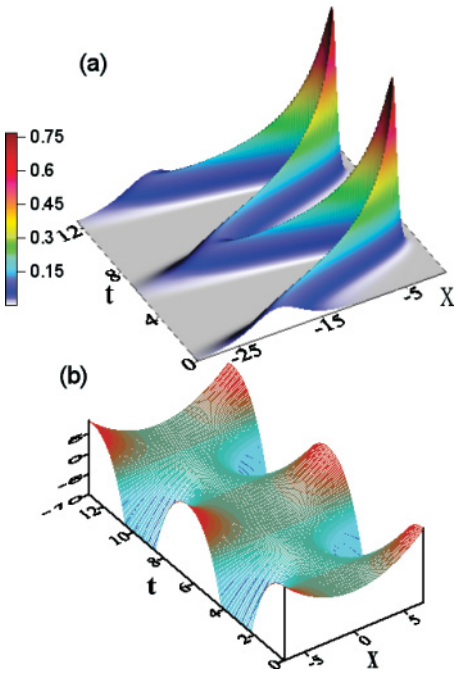

FIG. 5. (Color online) (a) Self-compression and periodical oscillations of a nonautonomous matter-wave soliton near the Feshbach resonance calculated within the framework of the model [Eqs. (49), (50)] after choosing the soliton management parameters $\beta = 0.75$, $\alpha = 0$, and $\omega = 0.5$. (b) Periodic sign-reversible oscillations of the external harmonic oscillator potential.

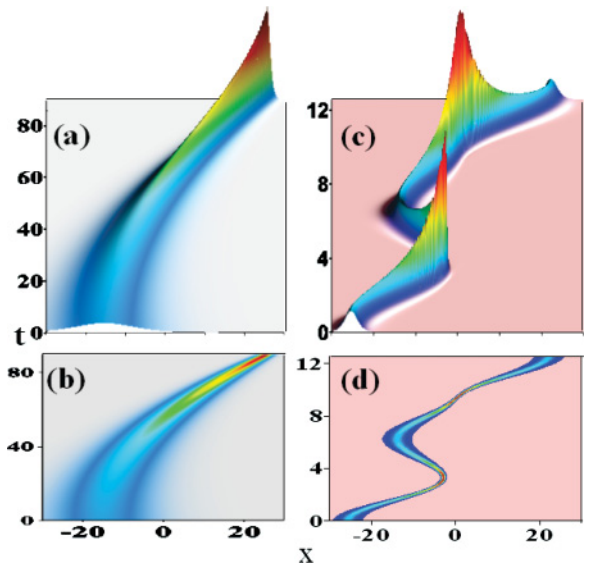

FIG. 6. (Color online) Evolution of nonautonomous matter-wave solitons calculated within the framework of the generalized model given by Eqs. (33), (49), and (50) after choosing the soliton-management parameters. (a,b) $\alpha = 0.01$, $\eta_0 = 0.1$, and $C_0 = 0.07$; (c,d) $\omega = 0.5$ and $\beta = 0.75$.

Without a resonance, under condition $C_0 = 0$, the solution of Eq. (52) reduces to that obtained by Chen and Liu in Ref. [16]:

$$\xi(x,t) = 2\eta_0(x + 2\kappa_0 t + \alpha_0 t^2 - x_0). \tag{54}$$

The Chen and Liu solution for negative initial velocity $\kappa_0 = -V_0$ ($V_0 > 0$) has the group velocity $v_g = 2(V_0 - \alpha_0 t)$ and travels toward the potential range with deceleration $2\alpha_0$ until the turning point $x_T = x_0 + V_0^2/\alpha_0$, where the velocity changes sign and the soliton is reflected back from the potential. Figure 6 shows that the deceleration effect preserves in the process of the nonautonomous soliton self-compression in the vicinity of the Feshbach resonance as well.

The generalized Satsuma and Yajima formula for eigenvalues $\eta_{01} = 1/2$, $\eta_{02} = 3/2$ can be regarded as a special case. In this case we find

$$\begin{aligned} Q_2(x,t) &= \frac{4}{\sqrt{(1-C_0t)}} \exp\left(-\frac{i}{2}\frac{C_0x^2}{1-C_0t}\right) \\ &\times \exp\left\{\left[-2\alpha_0 xt + \alpha_0 C_0 x t^2 \right.\right. \\ &\left.\left. - \alpha_0^2\left(\frac{2}{3}t^3 - \frac{1}{6}C_0t^4\right)\right](1-C_0t)^{-1}\right\} \\ &\times \frac{\exp(it/2/(1-C_0t) - \chi_{01})}{\cosh 4X + 4\cosh 2X - 3\cos[4t/(1-C_0t) + \Delta\varphi]} \\ &\times \{\cosh 3X - 3\cosh X \exp[i4t/(1-C_0t) - \Delta\varphi]\}, \end{aligned} \tag{55}$$

where $X(x,t) = (x - x_0 + \alpha_0 t^2)(1 - C_0 t)^{-1}$, $\Delta\varphi = \chi_{02} - \chi_{01}$.

Figure 7 shows examples of the bound nonautonomous solitons dynamics calculated in the framework of Eq. (53) for various values $\Delta\varphi = \chi_{02} - \chi_{01}$ and $\Delta x = x_{01} - x_{02}$.

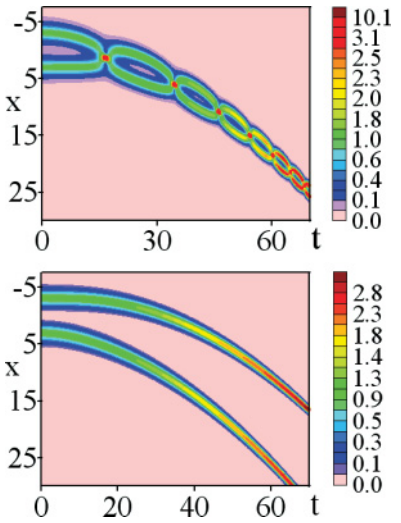

FIG. 7. (Color online) Nonlinear interaction of two nonautonomous solitons calculated within the framework of the generalized model given by Eq. (55) after choosing the soliton management parameters $\alpha = 0.01$, $C_0 = 0.01$, and $\eta_{01} = \eta_{02} = 1.0$. The relative phase difference between solitons is $\Delta\varphi = 0$ in the top panel but it is changed to $\Delta\varphi = \pi$ in the bottom panel.

The interesting part of the soliton interaction scenario in this case is connected with suppression of interaction forces among initially strongly overlapping solitons. An acceleration of the period of oscillation of a two-soliton pair, as well as the suppression of interaction, are clearly shown in Fig. 7. Consequently, similar to the canonical soliton case, the nonautonomous solitons in confining harmonic and linear x-dependent potentials attract or repel each other depending on their relative phase difference. Their pure solitonlike features (elastic character of interaction) are confirmed by accurate direct computer simulations.

V. VALIDITY OF 1D APPROXIMATION AND MATTER-WAVE SOLITON COLLAPSE INDUCED BY 1D-TO-3D TRANSFORMATIONS OF TRAPPING POTENTIALS

When studying the effects of nonlinear matter-wave management, we must also consider the validity of the GP model in this limit. Obviously, when the scattering length is varied with time, the dimensionless parameter controlling the validity of the mean-field approach [2–4] will be dependent on time, too:

$$n_{3D}|a_s(t)|^3 \ll 1, \tag{56}$$

where n_{3D} is the average density of the 3D dilute Bose gas. The inequality Eq. (56) means that BEC is sufficiently dilute for the effective range of the two-body interaction potential to be much smaller than the mean particle separation. Typical values of density range from 10^{13} cm^{-3} to 10^{15} cm^{-3}, so that $n_{3D}|a_s|^3$ is always less than 10^{-3} for a typical alkali-metal gas characterized by scattering length $a_{s0}(t=0) = 100a_0$ in units of the Bohr radius $a_0 = 0.0529$ nm. The relationship presented in Fig. 1 breaks down only in the extreme vicinity of the resonance, affording a large range of the density n_{3D} for which the GPE model is still appropriate. If we consider a typical condensate of density

from $n_{3D} = 10^{13}$ cm^{-3} to 10^{15} cm^{-3} and $a_{s0}(t=0) = 5$ nm so that parameter $n_{3D}|a_s(t=0)|^3$ varies from 1.25×10^{-6} to 1.25×10^{-4}, the GP equation is still valid when a_s is one order of magnitude larger $a_s(t=t_1) = 10a_{s0}(t=0) = 1000a_0 = 52.9$ nm, so that parameter $n_{3D}|a_s(t=0)|^3$ varies from 1.25×10^{-3} to 1.25×10^{-1} (see Fig. 1).

Let us consider the mean-field dynamics of the condensate when the main criterion [Eq. (56)] for validity of the GP equation is satisfied. Our goal now is to obtain the accurate criteria for adiabaticity of the matter-wave-management scenario:

$$\frac{1}{a_s}\frac{da_s}{dt} \approx \frac{1}{B_0 - B(t)}\frac{dB}{dt} \ll \frac{1}{T_{\text{eff}}}, \tag{57}$$

$$\frac{1}{\Omega_{\text{ho}}}\frac{d\Omega_{\text{ho}}}{dt} \ll \frac{1}{T_{\text{eff}}}, \tag{58}$$

where T_{eff} denotes an effective time scale of the atom-cloud variations. Equations (57) and (58) mean that both scattering length $a_s(t)$ and trapping potential $V(\mathbf{r}, t) = 1/2m\Omega_{\text{ho}}^2(t)\mathbf{r}^2$ are slowly varying functions of time as compared with $\exp(t/T_{\text{eff}})$.

The starting point of our study is the time-dependent 3D GP equation (GPE) for the complex wave function $\Psi(x, y, z, t)$ that describes the behavior of a BEC atom cloud in the 3D harmonic trapping potential:

$$i\hbar\frac{\partial\Psi}{\partial t} = -\frac{\hbar^2}{2m}\triangle\Psi + \frac{4\pi\hbar^2 a_s(t)}{m}|\Psi|^2\Psi + \frac{1}{2}m\Omega_{\text{ho}}^2(t)(x^2+y^2+z^2)\Psi. \tag{59}$$

As is well known, the GPE provides an excellent model of mean-field effects in BECs and has accurately predicted the onset of collapse of an attractive BEC. The basic GPE (59) is insufficient to study the collapsing condensate in the immediate vicinity of the Feshbach resonance where high-order effects become considerable. In the immediate vicinity of the Feshbach resonance, given by the empirically derived expression [Eq. (8)], the BEC collapses onto itself and its atoms form molecules due to three-body recombination [1–4]. That is why, in addition to the mean-field potential, a three-body recombination should be explicitly included in the GP equation as an imaginary loss term $-i\hbar K_3|\Psi(r,t)|^4/2$ [44]. Nonlinear atom losses are important for collapsing condensates when the magnetic fields are such that the Feshbach resonance is crossed. It would be expected that dissipative losses would be stronger only in the extreme vicinity of the resonance when the atom density becomes $n \approx 8\pi\hbar a_s/mK_3 \approx 10^{16}$ cm^{-3} for a typical alkali-metal gas [44]. However, in the present work, we only consider the parameter region where the scattering length does not change its sign, which means that the resonance is never crossed.

It should be emphasized that the adiabaticity criteria in soliton physics have been studied extensively both in theory and in experiments, particularly in connection with the development of adiabatic soliton perturbation methods and adiabatic optical soliton compression technique in dispersion-decreasing fibers [23–29]. Moreover, the criteria of adiabaticity for nonlinear matter waves have been considered recently within the context of atomic matter waves tunneling from macroscopically populated optical standing-wave traps and for BEC in a box whose size varies with time [45].

Following the ideas and method of Band, Malomed, and Trippenbach, let us show that a temporally varying 3D condensate wave function $\Psi(\mathbf{r}, t)$ is governed by four characteristic response times, $T_{\text{eff}} \div \{T_{\text{kin}}; T_{\text{int}}; T_{\text{trap}}; T_{\text{ho}}\}$, which can be formally obtained from the definition

$$\frac{1}{T_{\text{eff}}} = \frac{1}{\Psi(\mathbf{r}, t)}\frac{\partial\Psi(\mathbf{r}, t)}{\partial t}. \tag{60}$$

Note in particular that characteristic response times $T_{\text{eff}} \div \{T_{\text{kin}}; T_{\text{int}}; T_{\text{trap}}; T_{\text{ho}}\}$ are related throughout the kinetic energy (E_{kin}), atomic interaction energy (E_{int}), and external trapping potential energy (E_{trap}) variations. The response time scale $T_{\text{ho}} = 2\pi/\Omega_{\text{ho}}$ is the standard period of harmonic oscillations.

By using the equation for the characteristic size of an atomic 3D cloud,

$$\frac{1}{r_0^2} = -\left[\frac{1}{\Psi}\frac{\partial^2\Psi}{\partial\mathbf{r}^2}\right]_{\mathbf{r}=0}, \tag{61}$$

we obtain the important relations for characteristic response times of the problem,

$$T_{\text{kin}} = \frac{2mR_0^2}{\hbar} = \frac{2r_0^2}{\Omega_{\text{ho}}a_{\text{ho}}^2} = T_{\text{ho}}\frac{r_0^2}{\pi a_{\text{ho}}^2}, \tag{62}$$

$$T_{\text{int}} = \frac{m}{4\pi\hbar|a_s|n} = \frac{2a_{\text{hl}}^2}{\Omega_{\text{ho}}a_{\text{ho}}^2} = T_{\text{ho}}\frac{a_{\text{hl}}^2}{\pi a_{\text{ho}}^2}, \tag{63}$$

$$T_{\text{trap}} = \frac{2\hbar}{m\Omega_{\text{ho}}^2R_0^2} = \frac{2a_{\text{ho}}^2}{\Omega_{\text{ho}}r_0^2} = T_{\text{ho}}\frac{a_{\text{ho}}^2}{\pi r_0^2}, \tag{64}$$

where $a_{\text{ho}} = (\hbar/m\Omega_{\text{ho}})^{1/2}$ is the oscillator length of the harmonic potential, and $a_{\text{hl}}^2 = 1/(8\pi|a_s|n)$ is the healing length.

One can see that two response times T_{kin} and T_{trap} are related by two expressions,

$$T_{\text{trap}} \times T_{\text{kin}} = \frac{4}{\Omega_{\text{ho}}^2} = \frac{T_{\text{ho}}^2}{\pi^2}, \tag{65}$$

$$\frac{T_{\text{kin}}}{T_{\text{trap}}} = \frac{r_0^4}{a_{\text{ho}}^4}, \tag{66}$$

two response times T_{kin} and T_{int} are related by

$$\delta = \frac{T_{\text{kin}}}{T_{\text{int}}} = \frac{r_0^2}{a_{\text{hl}}^2}, \tag{67}$$

and the next two response times T_{trap} and T_{int} are related by

$$\frac{T_{\text{trap}}}{T_{\text{int}}} = \frac{a_{\text{ho}}^4}{a_{\text{hl}}^2r_0^2} = \delta\frac{a_{\text{ho}}^4}{r_0^4}. \tag{68}$$

The qualitative behavior of condensate depends on the value of the dimensionless parameter δ. If δ is small, $\delta \ll 1$, then the interatomic interaction is just a small perturbation on the noninteracting Bose gas behavior. In the linear approximation $\delta \ll 1$, the statement $a_s(0) = 0$, is formally equivalent to setting $T_{\text{kin}} = T_{\text{trap}}$, and the size of the atomic cloud is determined by $r_0 = a_{\text{ho}}$. In the opposite case, when $\delta \approx 1$, and without a trapping potential $V_{\text{ext}}(r, t) = 0$, the atomic cloud

behavior is determined primarily by the competition between the interaction-energy term and the kinetic-energy term. In the case of attractive self-interactions, when the scattering length $a_s(0)$ is negative, the two energies are equal when $T_{\rm kin} = T_{\rm int}$ and the characteristic radius of the atomic cloud is of the order of the healing length $r_0 = a_{\rm hl}$. In particular, in 3D world, $\delta = 1$ when

$$\frac{T_{\rm kin}}{T_{\rm int}} = 8\pi n|a_s|r_0^2 = \frac{6\,N\,|a_s|}{r_0} = 1, \tag{69}$$

where N is the total number of atoms in the volume $4/3\pi r_0^3$. If we consider a typical alkali-metal gas with $a_{s0} = 5.0$ nm in a harmonic trap with $r_0 = 30$ μm, we obtain $N = 10^3$ atoms trapped in a solitary matter wave under condition $T_{\rm int} = T_{\rm kin}$. In the general case, the condensate behavior is determined by the competition of the external, interatomic, and kinetic potentials. Collapse of the 3D BEC system occurs when N exceeds a critical value $N_{\rm cr}$, which is given by $N_{\rm cr} = 0.67r_0/|a_s|$ [2–4]. This implies that for the example considered here, there exists a critical number of atoms $N_{\rm cr} = 4 \times 10^3$ beyond which a collapse occurs.

According to Eqs. (57) and (58), the soliton behavior is adiabatic when the main parameters of the system, such as trapping potential and nonlinearity, vary slowly relative to the time scale $T_{\rm eff} = T_{\rm int}$:

$$\frac{1}{B_0 - B(t)}\frac{dB}{dt} \ll \Omega_{\rm ho}\frac{a_{\rm ho}^2}{2a_{\rm hl}^2};\ \frac{1}{\Omega}\frac{d\Omega}{dt} \ll \Omega_{\rm ho}\frac{a_{\rm ho}^2}{2a_{\rm hl}^2}. \tag{70}$$

The characteristic quantum-mechanical length scale $a_{\rm ho}$ may be written in a very useful form proposed by Pethick and Smith in [2],

$$a_{\rm ho} \approx 10.1\left(\frac{100\ {\rm Hz}}{f_{\rm ho}}\frac{1}{A}\right)^{1/2}\mu{\rm m}, \tag{71}$$

in terms of the trap frequency $f_{\rm ho} = \Omega_{\rm ho}/2\pi$ measured in Hz and the mass number A, namely, the number of nucleons in the nucleus of the atom. For example, when $f_{\rm ho}A \approx 100$, the relationship in Eq. (71) means that $a_{\rm ho} \approx 10$ μm. In the case illustrated in Fig. 1, when $f_{\rm ho}A = 100$, we obtain $A = 85$ and $f_{\rm ho} = 1.18$ Hz, and one can find the following estimation for characteristic time scale: $T_{\rm eff} = 2.5$ ms. That is why our adiabatic matter-wave soliton self-compression scenario is still valid as long as the speed of the field ramp $\gamma = dB/dt$ is low enough $\gamma = dB/dt \ll 3$ G/ms. In a harmonically trapped BEC with time-varying frequency $\Omega_{\rm ho}(t)$, a total frequency sweep value $d\Omega_{\rm ho}/dtT_{\rm eff}$ during a time scale $T_{\rm eff}$ should be small enough compared to a trapping potential frequency $\Omega_{\rm ho}$, namely, $d\Omega_{\rm ho}/dtT_{\rm eff} \ll \Omega_{\rm ho}$. For a characteristic time scale $T_{\rm eff} = 2.5$ ms and $f_{\rm ho} = 1.18$ Hz, we obtain the following adiabaticity criterion: $df_{\rm ho}/dt \ll 0.5$ kHz s^{-1}.

In the strict sense, canonical NLSE solitons exist only in the 1D world [39]. Physically, the existence of 1D solitons indicates the fundamental feature of the 1D NLSE model: its complete integrability [39]. That is why the quasi-1D (a cigar-shaped) geometry was used in all pioneering and recent experiments with matter-wave solitons [5–11]. It is a well-established fact that beyond the 1D world, disk-shaped (2D) and ball-shaped (3D) solitary waves are unstable due to transverse perturbations and collapse [2–4]. For example, temporal periodic modulation of the scattering length in 2D disk-shaped BECs was shown to excite Faraday patterns in the atom density in the plane transverse to the tight confinement direction [46].

Let us consider a cylindrically symmetric harmonic trapping potential,

$$V(x, y, z, t) = \tfrac{1}{2}m\Omega_{\rm ho\|}^2(t)\,x^2 + \tfrac{1}{2}m\Omega_{\rm ho\perp}^2(y^2 + z^2), \tag{72}$$

with constant radial trap frequency $\Omega_{\rm ho\perp}$ and a varying-in-time longitudinal one $\Omega_{\rm ho\|}(t)$,

$$\Omega_{ho\|}^2(t) = \Omega_{ho\|}^2(t = 0) \times \Omega^2(t), \tag{73}$$

where dimensionless function $\Omega^2(t)$ describes the time-varying trapping potential only in the axial direction x, so that a transverse trap does not depend on time $\Omega_{\rm ho\perp} = {\rm const}$.

Nonlinear dynamics of a quasi-1D (a cigar-shaped) condensate under much greater transverse than axial confinement $\Omega_{\rm ho\|}^2 \ll \Omega_{\rm ho\perp}^2$ can be considered in the framework of the GPE,

$$i\hbar\frac{\partial\Psi}{\partial t} = -\frac{\hbar^2}{2m}\triangle\Psi + \frac{4\pi\hbar^2 a_s(t)}{m}\,|\Psi|^2\,\Psi + \frac{1}{2}m\Omega_{\rm ho\|}^2(t)\,x^2\Psi + \frac{1}{2}m\Omega_{\rm ho\perp}^2(y^2 + z^2)\Psi, \tag{74}$$

with factorized wave function

$$\Psi(\mathbf{r}, t) = \Xi(\mathbf{r}_\perp, t)\psi(x, t) \tag{75}$$

separating transverse ($r_\perp^2 = y^2 + z^2$) and longitudinal (x) dependencies [2–4]. The 3D GP equation (74) can be reduced to a 1D model if one can neglect excitations of higher-order transverse modes so that the atoms occupy only the ground state of their transverse motion. The wave function separation (75) can be achieved formally by a two-time-scale expansion with a slow-response time scale $T_{\rm trap\|}$ and a fast-response time scale $T_{\rm trap\perp}$ given by

$$T_{\rm trap\|} = \frac{2\hbar}{m\Omega_{\rm ho\|}^2 r_0^2} = \frac{2a_{\rm ho\|}^2}{\Omega_{\rm ho\|}r_0^2} = T_{\rm ho\|}\frac{a_{\rm ho\|}^2}{\pi r_0^2}, \tag{76}$$

$$T_{\rm trap\perp} = \frac{2\hbar}{m\Omega_{\rm ho\perp}^2 r_0^2} = \frac{2a_{\rm ho\perp}^2}{\Omega_{\rm ho\perp}r_0^2} = T_{\rm ho\perp}\frac{a_{\rm ho\perp}^2}{\pi r_0^2}. \tag{77}$$

Although in a strict sense this separation can be done only in the linear problem, the effective 1D nonlinear coefficient appears to be a factor in the nonlinear term resulting from the subsequent transverse integration:

$$G_{\rm 1D}(t) = \frac{\int\int_{-\infty}^{\infty} G_{\rm 3D}(t)\Xi^4(y, z)dydz}{\int\int_{-\infty}^{\infty}\Xi^2(y, z)dydz}. \tag{78}$$

The averaging procedure Eq. (78), in full analogy with the same procedure for optical solitons in fibers [23–26], leads to $G_{\rm 1D}(t) = 2\hbar^2 a_s(t)/(ma_{\rm ho\perp}^2)$, where $a_{\rm ho\perp}$ is the transverse harmonic oscillator length. Physically, transition to the quasi-1D description is possible if the change of the chemical potential due to the mean-field interaction is much smaller than the level spacing in the transverse trapping potential [2–4].

The net result is the 1D GP equation

$$i\hbar\frac{\partial}{\partial t}\psi(x,t) = -\frac{\hbar^2}{2m}\frac{\partial^2\psi}{\partial x^2} + \frac{2\hbar^2 a_s(t)}{m a_{\mathrm{ho}\perp}^2}\,|\psi(x,t)|^2\,\psi + \frac{1}{2}m\Omega_{\mathrm{ho}\|}^2(t)x^2\psi(x,t), \tag{79}$$

where $\psi(x,t)$ is the quasi-1D wave function normalized to the number of particles. By using the following transformations of functions and coordinates,

$$Q(x,t) \to \sqrt{\frac{a_{\mathrm{ho}\|}}{N}}\psi(x,t); t \to \Omega_{\mathrm{ho}\|}t; x \to x/a_{\mathrm{ho}\|}, \tag{80}$$

$$R(t) \to \varepsilon a_s(t)\left(\frac{a_{\mathrm{ho}\|}}{a_{\mathrm{ho}\perp}}\right)^2, \tag{81}$$

where $\varepsilon = 2a_s(0)N/a_{\mathrm{ho}\|}$, Eq. (78) can be reduced to the generalized GPE model (21) with varying-in-time nonlinearity and confining parabolic potential:

$$i\frac{\partial Q}{\partial t} + \frac{1}{2}\frac{\partial^2 Q}{\partial x^2} + \sigma R(t)\,|Q|^2\,Q - \frac{1}{2}\Omega^2(t)x^2 Q = 0. \tag{82}$$

The transition from 3D to 1D geometry demonstrates once again the parallels between two theoretical methods developed in the BEC theory [2–4] and in nonlinear fiber optics [23–26].

The exact integrability conditions given by Eqs. (22) and (23) establish a one-to-one correspondence between varying-in-time nonlinearity and parabolic trapping potential. Because of this, the interested reader can take different control functions $R(t)$ to find both corresponding trapping potentials from Eq. (23) and soliton solutions by using the algorithm [Eqs. (25)–(32)] developed in this article. Let us show for example, that the so-called Miura transformation in the soliton theory (see, for example, [23]),

$$\Omega^2(t) = \frac{\partial\Upsilon}{\partial t} - \Upsilon^2(t), \tag{83}$$

allows one to obtain simple particular analytic solutions for $R(t)$ given by

$$R(t) = \exp\left[\int^t \Upsilon(t')dt'\right], \tag{84}$$

where $\Upsilon(t)$ is an arbitrary integrable function.

Now we turn our attention to finding specified conditions for nonlinear soliton management by means of the Feshbach resonance.

When $\Upsilon(t) = \gamma = \mathrm{const}$, the conditions of compatibility for nonlinearity and parabolic potential are given by

$$R(t) = \exp(\gamma t); \quad \Omega^2(t) = -\gamma^2, \tag{85}$$

which represents the repulsive character of parabolic potential for all times.

In the case of algebraic functions $\Upsilon(t)$, there exists the following set of interesting compatibility conditions:

$$\Upsilon(t) = \frac{\gamma}{1+\gamma t}; \quad R(t) = 1+\gamma t; \quad \Omega^2(t) = -\frac{2\gamma^2}{(1+\gamma t)^2}, \tag{86}$$

$$\Upsilon(t) = -\frac{\gamma}{1+\gamma t}; \quad R(t) = \frac{1}{1+\gamma t}; \quad \Omega^2(t) = 0, \tag{87}$$

$$\Upsilon(t) = -\frac{2\gamma t}{1+\gamma t^2}; \quad R(t) = \frac{1}{1+\gamma t^2}; \quad \Omega^2(t) = -\frac{2\gamma}{1+\gamma t^2}. \tag{88}$$

It is important to note that for linearly increasing (positive γ) or decreasing (negative γ) in the time control function $R(t)$ given by Eq. (86), the character of harmonic potential remains repulsive for all times, as it is in the case of exponentially increasing nonlinearity [Eq. (85)]. The case of hyperbolic increase (negative γ) or decrease (positive γ) in time nonlinearity $R(t)$ (87) denotes that the confining harmonic potential is vanishing and the matter-wave soliton can be stabilized even without a trapping potential. The last case [Eq. (88)], presents one of the most interesting possibilities. With negative γ, the parabolic potential remains attractive for all times but its localization region decreases progressively with time [see Eq. (88)].

In the case of periodically varying magnetic field $B(t) = \beta\cos(\varpi t)$, the spectral parameter $\Lambda(t)$ of the IST method is directly related to the magnetic field variations. Now the control function $R(t)$ is a trigonometric periodically varying function. Consequently, one can find from Eqs. (83) and (84) the following set of compatibility conditions:

$$\Upsilon(t) = \gamma_2\varpi_2\cos(\varpi_2 t); \quad R(t) = \exp[\gamma_2\sin(\varpi_2 t)]; \quad \Omega^2(t) = -\gamma_2\varpi_2^2[\sin(\varpi_2 t) + \gamma_2\cos^2(\varpi_2 t)], \tag{89}$$

$$\Upsilon(t) = \frac{\gamma_2\varpi_2\cos(\varpi_2 t)}{1+\gamma_2\sin(\varpi_2 t)}; \quad R(t) = 1+\gamma_2\sin(\varpi_2 t); \quad \Omega^2(t) = -\frac{\{\gamma_2\varpi_2^2\sin(\varpi_2 t)[1-\gamma_2\sin(\varpi_2 t)] + 2\gamma_2^2\varpi_2^2\}}{[1+\gamma_2\sin(\varpi_2 t)]^2}, \tag{90}$$

$$\Upsilon(t) = -\frac{\gamma_2\varpi_2\cos(\varpi_2 t)}{1+\gamma_2\sin(\varpi_2 t)}; \quad R(t) = \frac{1}{1+\gamma_2\sin(\varpi_2 t)}; \quad \Omega^2(t) = \frac{\gamma_2\varpi^2\sin\varpi t}{1+\gamma_2\sin\varpi t}, \tag{91}$$

In the case of hyperbolic functions $\Upsilon(t)$, one may find the following set of relations between nonlinear control functions $R(t)$ and trapping potential, which are interesting from the practical point of view:

$$\Upsilon(t) = -\gamma_3\tanh(\gamma_3 t); \quad R(t) = \mathrm{sech}(\gamma_3 t); \quad \Omega^2(t) = -\gamma_3^2, \tag{92}$$

$$\Upsilon(t) = \gamma_3\mathrm{sech}^2(\gamma_3 t); \quad R(t) = \exp[\tanh(\gamma_3 t)]; \quad \Omega^2(t) = -\gamma_3^2\mathrm{sech}^2(\gamma t)\{[\tanh(\gamma_3 t)+1]^2 - 2\}. \tag{93}$$

Equation (92) can be considered as the solitary barrierlike variations of the nonlinearity. The last example [Eq. (93)] illustrates the effect of the nonlinearity saturation.

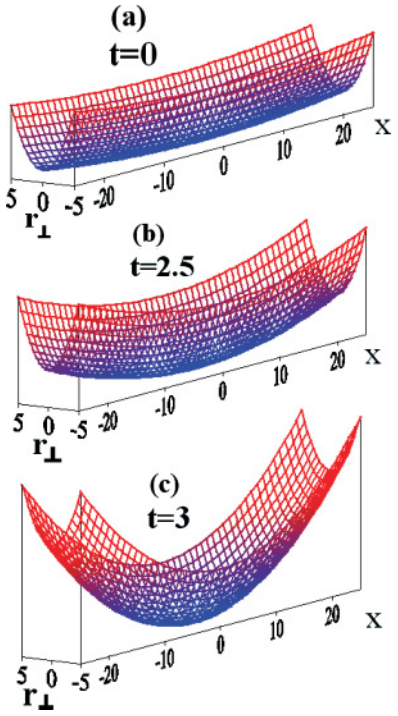

FIG. 8. (Color online) The reverse process of 1D-to-3D transformation from cigar-shaped geometry to ball-shaped geometry of trapping potential $V(r,t) = \varkappa^2\Omega^2(t)x^2/2 + r_\perp^2/2$ under the exact integrability conditions given by Eq. (88) with negative $\gamma = -0.1$ at different time scales. (a) $t = 0$, (b) $t = 2.5$, (c) $t = 3.0$, after choosing the aspect ratio $\varkappa^2 = 0.04$ ($r_\perp^2 = y^2 + z^2$).

It is easy to understand that as a consequence of varying-in-time nonlinearity and trapping potential given, in particular, by Eqs. (85)–(93), the atom cloud is subjected to wide axial variations, including its self-compression, and in general it may be that the initially quasi-1D cigar-shaped structure of the atom cloud transforms continuously to the ball-shaped 3D structure. That is why the reverse process of 1D-to-3D transformation from cigar-shaped to ball-shaped geometry can be observed because of the soliton self-compression effect. This is crucial for the purposes of matter-wave soliton management under the exact integrability conditions [Eqs. (22), (23)] and, in particular, the examples considered in Eqs. (85)–(93).

For better visualization of these ideas, we present here three examples of such reverse and nontrivial 1D-to-3D transformations (see Figs. 8–11 for details). Figure 8 shows the trapping harmonic potential of the exactly integrable nonautonomous system given by Eqs. (88) with negative γ. To be specific, we show in Fig. 9 all control functions $R(t)$ and $\Omega(t)$ for this case, so that Figs. 8 and 9 are probably the most dramatic direct manifestations of the reverse 1D-to-3D transformations of a trapping potential.

Figure 10 shows an example of periodic sign-reversible variations in time of the confining potential (periodic-in-time repulsive and attractive parabolic potentials) which have been calculated according to the exact integrability conditions given by Eqs. (89). And, finally, Fig. 11 represents the results of periodic 1D-to-3D transformations from attractive cigar-shaped to repulsive ball-shaped structures that have

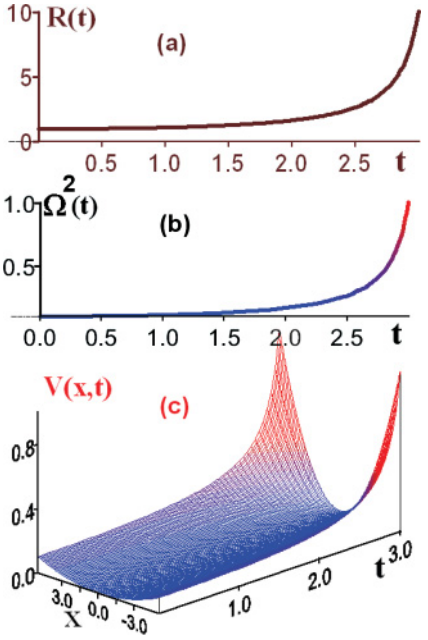

FIG. 9. (Color online) Main soliton-management functions (a) $R(t)$, (b) $\Omega^2(t)$, and (c) axial trapping potential varying in time under the exact integrability conditions given by Eq. (88) after choosing the aspect ratio $\varkappa^2 = 0.04$ of trapping potential $V(r,t) = \varkappa^2\Omega^2(t)x^2/2 + r_\perp^2/2$ and $\gamma = -0.1$.

been calculated in the framework of the exact integrability conditions given by Eqs. (49) and (50).

It should be emphasized that all soliton solutions presented in the Secs. II and III are strictly valid for the limiting case of 1D condensate. That is why it is natural to ask to what extent it is possible to consider the general solution for the condensate

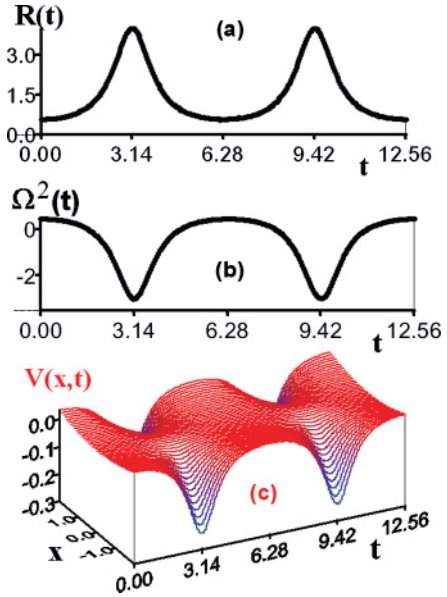

FIG. 10. (Color online) Main soliton-management functions (a) $R(t)$, (b) $\Omega^2(t)$, and (c) axial trapping potential varying in time under the exact integrability conditions given by Eqs. (89) after choosing the aspect ratio $\varkappa^2 = 0.04$ of trapping potential $V(r,t) = \varkappa^2\Omega^2(t)x^2/2 + r_\perp^2/2$ and $\varpi = 1.0$.

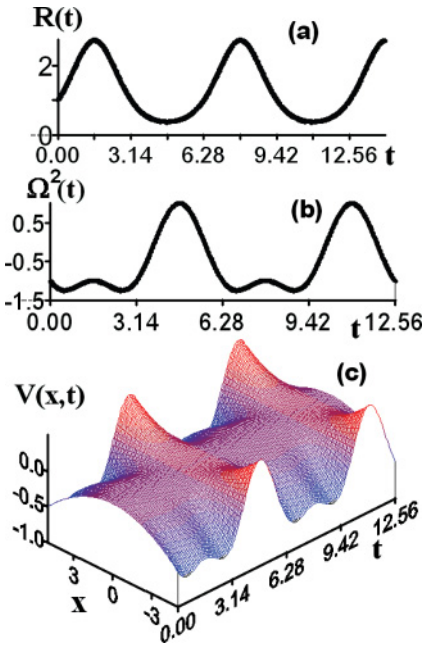

FIG. 11. (Color online) Main soliton management functions (a) $R(t)$, (b) $\Omega^2(t)$, and (c) axial trapping potential varying in time under the exact integrability conditions given by Eqs. (49) and (50) $R(t) = (1+\beta\cos\varpi t)^{-1}$, $\Omega^2(t) = \beta\varpi^2\cos\varpi t/(1+\beta\cos\varpi t)$ after choosing the aspect ratio $\varkappa^2 = 0.04$ of trapping potential $V(r,t) = \varkappa^2\Omega^2(t)x^2/2 + r_\perp^2/2$, $\beta = 0.75$, and $\varpi = 1.0$.

density $n(\mathbf{r},t)$ in the factorized form,

$$\frac{n(\mathbf{r},t)}{n_0} = \frac{|\Psi(\mathbf{r},t)|^2}{|\Psi(\mathbf{r}=0,t=0)|^2} = \frac{[1-\Phi(0)]^2}{[1-\Phi(t)]}\mathrm{sech}^2\left\{\frac{x}{L_{\mathrm{sol}\|}}\frac{[1-\Phi(0)]}{[1-\Phi(t)]}\right\} \times \exp\left(-\frac{y^2+z^2}{L_\perp^2}\right), \tag{94}$$

where $|\Psi(\mathbf{r},t)|^2/|\Psi(\mathbf{r}=0,t=0)|^2 \equiv n(\mathbf{r},t)/n_0$ is the density of atoms at the point in question normalized to its initial peak value $n_0 = N/(2\pi L_\perp^2 L_{\mathrm{sol}\|})$, and $L_\perp$ and $L_{\mathrm{sol}\|}$ are the initial radial and axial widths of the wave function [see Fig. 12(a)].

In Eq. (94), the exact 1D soliton solution [Eq. (25)] has been chosen for the longitudinal direction, whereas in the transverse direction a Gaussian ansatz is the optimal one. To reveal the basic properties of 3D matter-wave solitary waves, we have solved numerically the nonautonomous GP equation [Eq. (74)] by applying an operator-splitting method based on 3D fast Fourier transform (FFT) which, since its discovery by Feit and Fleck [47], is a well-developed computational method in nonlinear optics, acoustics, and self-focusing theory. The condition of validity of 1D soliton self-compression [Eq. (29)] has been tested by solving Eq. (74) with initial conditions given by Eq. (94) and taking as the managing functions $R(t)$ and $\Omega_{\mathrm{ho}\|}^2(t)$ several profiles given by Eqs. (85)–(93).

In order to simulate an extremely strong 1D-to-3D transformation of the initially cigar-shaped cloud of atoms into the BEC bullet, the varying-in-time nonlinearity $R(t)$ was chosen as $R(t) = 1/(1-0.1t^2)$ in accordance with Eqs. (88). The initial state presents a cigar-shaped density of condensed $N = 10^3$ atoms with axial and radial sizes $L_{\mathrm{sol}\|} = 15$ μm and $L_\perp = 1.5$ μm, respectively, and with initial 3D peak density $n_0 = 0.5\times10^{13}$ cm^{-3}. Axial and radial trapping harmonic potential frequencies have been chosen as $\Omega_{\mathrm{ho}\perp} = 2\pi\times52$ Hz and $\Omega_{\mathrm{ho}\|} = 2\pi\times0.52$ Hz, respectively, and initial scattering length was chosen as $a_s(t=0) = -2a_0$ to simulate its increasing up to ten times $a_s(t=t_{\mathrm{fin}}) = -20a_0$ and to calculate corresponding self-compression of the atom cloud by a factor of ten.

The main results of computer simulations are presented in Fig. 12 at different dimensionless time scales: (a) $-t = 0$, (b) $-t = 2.25$, (c) $-t = 2.75$, and (d) $-t = 3.0$, which are normalized on $T_{\mathrm{int}} = 30$ ms and correspond to 67.5 ms (b), 82.5 ms (c), and 90 ms (d) in Fig. 12. In Figs. 12(a)–12(c), the condensate density $n(\mathbf{r},t)$ is normalized to the initial peak density value $n_0 = 0.5\times10^{13}$ cm^{-3}. Direct computer experimentation enables us to draw the following conclusions. First, our simulations confirm the quadratic in time soliton compression scenario at the initial stage of self-compression, in full accordance with analytical expressions Eqs. (29) and (32). Second, the essential finding in our simulations is that during the self-compression, the elongated soliton separates on two ball-shaped solitarylike structures. In Fig. 12, we show both a typical soliton self-compression scenario and the initial stage of soliton necking and splitting near the resonance time when the peak density rises dramatically with time [see Fig. 12(d)]. It is this effect that disrupts the solitonic structure of the atom cloud and breaks the effect of soliton adaptation to the external potential given by the exact integrability conditions [Eqs. (88)]. As a matter of fact, based on computer simulations, we conclude that a 1D nonautonomous GPE model accurately describes the matter-wave soliton self-compression until the axial $L_{\mathrm{sol}\|}$ and radial $L_\perp$ widths of a soliton satisfy the following "empirical" condition: $L_{\mathrm{sol}\|}^2(t) \gtrsim 3L_\perp^2$. Because of this, the main assumption based on the factorized form Eq. (94) holds true only within the limits $L_{\mathrm{sol}\|}^2(t) \gtrsim 3L_\perp^2$. By using the simplest approximation for a 1D soliton width in the quasi-1D BEC with varying-in-time scattering length,

$$L_{\mathrm{sol}\|}^2(t)n_{1\mathrm{D}}(t) \approx \frac{L_\perp^2}{4|a_s(t)|}, \tag{95}$$

where $n_{1\mathrm{D}}(t) = N/L_{\mathrm{sol}\|}(t)$ represents the 1D density of the condensate, we can find the following "empirical" condition of the validity of the 1D nonautonomous soliton concept, namely, the 1D nonautonomous matter-wave soliton [Eq. (25)] exists under exact integrability conditions [Eq. (82)] if and only if varying-in-time scattering length $a_s(t)$ and 1D density $n_{1\mathrm{D}}(t)$ satisfy the following inequality:

$$|a_s(t)|n_{1\mathrm{D}}(t) \lesssim 1/12 \approx 0.1. \tag{96}$$

To date, bright matter-wave solitons and trains of bright solitons have been studied in experiments with Bosonic lithium having attractive interactions [8,9]. The negative value of the scattering length for ^{7}Li prevents the formation of a condensate with more then a few thousand atoms [8,9]. If we consider the typical experimental conditions for the generation of

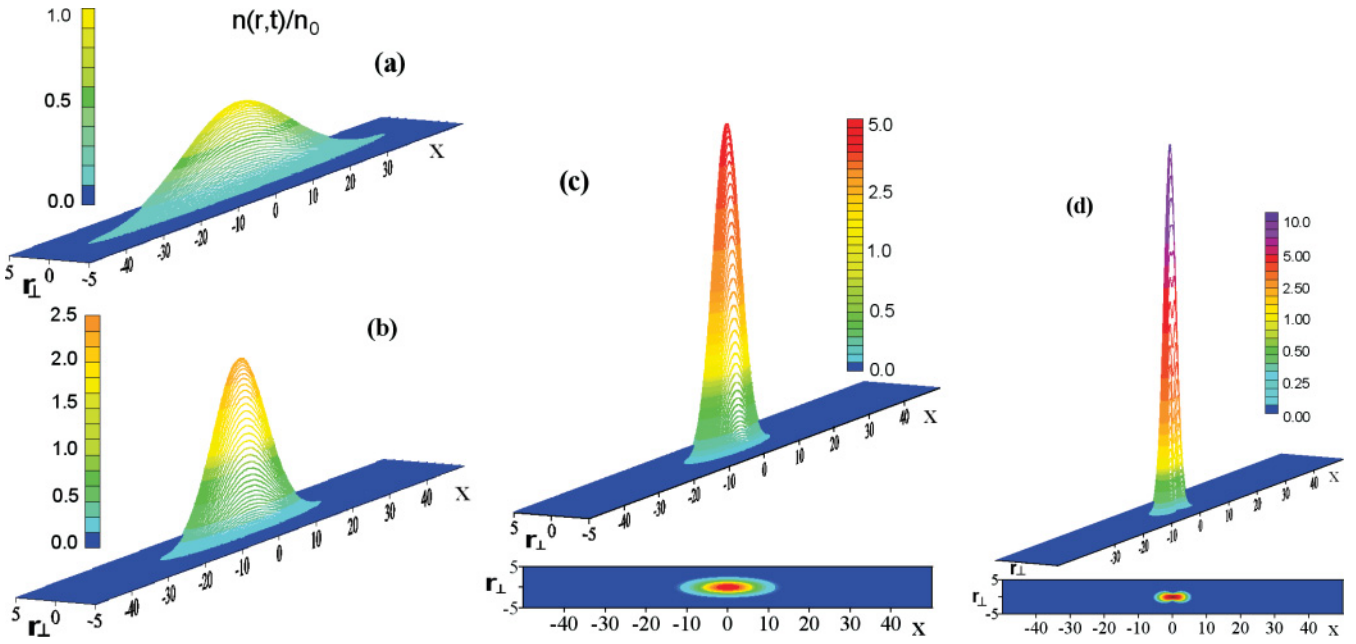

FIG. 12. (Color online) Self-compression of matter-wave soliton near the Feshbach resonance calculated within the framework of the nonautonomous GPE model (74) after choosing the soliton management functions $R(t) = (1 + \gamma t^2)^{-1}$ and $\Omega^2(t) = -2\gamma(1 + \gamma t^2)^{-1}$ with negative $\gamma = -0.1$ at different dimensional time scales normalized to $T_{\rm int} = 30$ ms. (a) $-t = 0$, (b) $-t = 2.25$, (c) $-t = 2.75$, and (d) $-t = 3.0$, which correspond to (b) 67.5 ms, (c) 82.5 ms, and (d) 90 ms. The initial state represents a quasi-1D cigar-shaped cloud of condensed $N = 10^3$ atoms with axial and radial sizes $L_{\rm sol\|} = 15$ μm and $L_\perp = 1.5$ μm, respectively. In all figures the condensate density $n(\mathbf{r}, t)$ is normalized to the initial peak value $n_0 = 0.5 \times 10^{13}$ cm^{-3}. Axial and radial widths are given in microns.

matter-wave solitary waves in quasi-1D ^{7}Li condensate [8,9] with typical radial width $a_{\rm ho\perp} = 1.0$ μm, we conclude that 1D approximation is still valid when the width of a compressed BEC soliton is of the order of $L_{\rm sol\|} = 1.7$ μm.

A more detailed description of our computer experiment will be provided in a separate presentation.

VI. CONCLUSIONS

In summary, we have studied the main features of nonautonomous matter-wave solitons near the Feshbach resonance with continuously tuned scattering length. We have focused on the situation in which the generalized 1D GPE model with varying nonlinearity was found to be exactly integrable from the point of view of the IST method. We stress that exact soliton solutions exist only under certain conditions and that varying-in-time nonlinearity and confining harmonic potential cannot be chosen independently; they satisfy the exact integrability conditions given by Eqs. (21)–(23). That means, in particular, that near the Feshbach resonance the matter-wave soliton can be stabilized even without a trapping potential. We have considered the two most physically important examples where the applied magnetic field varies in time linearly or periodically. In the case of periodically varying nonlinearity, variations of the external harmonic potential are found to be sign-reversible (periodic attractive and repulsive). We have investigated two bound soliton states and demonstrated their stability by means of direct computer experiments. The conditions of the validity of the nonautonomous soliton concept have been tested by solving general 3D GPE taking as the managing functions several profiles given by Eqs. (86)–(93). The interplay between the time-dependent nonlinearity and 1D-to-3D transformation of trapping potential leads to the necking and splitting of the elongated input soliton on two separate parts. It is this effect that disrupts the solitonic structure of the atom cloud and breaks the validity of 1D theory. Based on computer simulations, we have found that a 1D nonautonomous matter-wave soliton exists if and only if varying-in-time scattering length $a_s(t)$ and 1D density $n_{\rm 1D}(t)$ satisfy the following "empirical" condition: $|a_s(t)|n_{\rm 1D}(t) \lesssim 0.1$.

The results reported in this article are of general physics interest and offer many opportunities for further scientific studies. For example, the Feshbach resonance makes it possible to investigate experimentally the self-compression of bright and dark matter waves and realize the so-called nonlinear soliton pairing effect [10,48]. These states, often called "nonlinear pairing" or "symbiotic" solitons, have been considered for the first time in nonlinear optics [48].

Notice that in the real experiments with BEC, the trapping potential is not the harmonic oscillator potential extending to infinity but the truncated one. The interesting possibilities have been found for the autonomous GP model with the tanh-shaped potential in [49]. The problem of the nonautonomous soliton dynamics in the truncated potential remains open.

It should be emphasized that the nonautonomous NLSE model implies the existence of many fundamental nonlinear phenomena, independent of the physical origin of the nonlinearity and dispersion. The classification of dynamic systems into autonomous and nonautonomous is often convenient and can correspond to different physical situations in which, respectively, the external time-dependent driving force is

present or absent. If the system is subjected to some form of external time-dependent force $\gamma(t)$, the GPE model transforms to the following nonautonomous equation:

$$i\frac{\partial\psi}{\partial t}+\frac{1}{2}D(t)\frac{\partial^2\psi}{\partial x^2}+\left[\sigma G(t)|\psi|^2-2\alpha(t)x-\frac{1}{2}\Omega^2(t)x^2\right]\psi=\frac{i}{2}\gamma(t)\psi, \tag{97}$$

where the dispersion management function $D(t)$ is being introduced. The GPE model (97) becomes similar to Eq. (21),

$$i\frac{\partial Q}{\partial t}+\frac{1}{2}D(t)\frac{\partial^2 Q}{\partial x^2}+\left[\sigma R(t)|Q|^2-2\alpha(t)x-\frac{1}{2}\Omega^2(t)x^2\right]Q=0, \tag{98}$$

after the following transformations,

$$\psi(x,t)=Q(x,t)\exp\left[\frac{1}{2}\int_0^t\gamma(\tau)d\tau\right], \tag{99}$$

$$R(t)=G(t)\exp\left[\int_0^t\gamma(\tau)d\tau\right], \tag{100}$$

and all results obtained in the present article can be easily generalized for the case of the BEC with time-dependent loss or gain and with the self-induced soliton phase shift $\varphi(x,t)$ in Eq. (19) defined as $\varphi(x,t)=\Theta(t)x^2/2$,

$$\Theta(t)=-\frac{W[(R(t),D(t)]}{D^2(t)/R(t)}, \tag{101}$$

and dependent on the Wronskian $W(R,D)=RD_t'-DR_t'$.

The Lax equation (9) provides the nonautonomous model (98) under the condition that dispersion $D(t)$, nonlinearity $R(t)$ [dependent now on gain or loss according Eq. (100)], and the harmonic potential satisfy the following relations,

$$\Omega^2(t)D(t)=\frac{W(R,D)}{RD}\frac{d}{dt}\ln R(t)-\frac{d}{dt}\left[\frac{W(R,D)}{RD}\right] \tag{102}$$

$$=\frac{d}{dt}\ln D(t)\frac{d}{dt}\ln R(t)-\frac{d^2}{dt^2}\ln D(t)-R(t)\frac{d^2}{dt^2}\frac{1}{R(t)} \tag{103}$$

$$=D(t)\frac{d}{dt}\left[\frac{\gamma(t)}{D(t)}\right]-\gamma^2(t)+\left[2\gamma(t)+\frac{d}{dt}\ln G(t)\right]\frac{W(G,D)}{GD}-\frac{d}{dt}\left[\frac{W(G,D)}{GD}\right] \tag{104}$$

$$=D(t)\frac{d}{dt}\left[\frac{\gamma(t)}{D(t)}\right]-\gamma^2(t)+\left[2\gamma(t)+\frac{d}{dt}\ln G(t)\right]\frac{d}{dt}\ln\frac{D(t)}{G(t)}-\frac{d^2}{dt^2}\ln\frac{D(t)}{G(t)}, \tag{105}$$

and the eigenvalues are given by

$$\Lambda(t)=\kappa(t)+i\eta(t)=\frac{D_0R(t)}{R_0D(t)}\left[\Lambda(0)+\frac{R_0}{D_0}\int_0^t\frac{\alpha(\tau)D(\tau)}{R(\tau)}d\tau\right], \tag{106}$$

where the time-invariant eigenvalues $\Lambda(0)=\kappa_0+i\eta_0$, $D_0=D(0)$, and $R_0=R(0)$ are defined by the initial conditions. Equations (102)–(105) are presented here in four different representative forms, where $W(G,D)=GD_t'-DG_t'$. Two Wronskians $W(R,D)$ and $W(G,D)$ are related by $W(R,D)=\exp[\int_0^t\gamma(\tau)d\tau][W(G,D)+D(t)G(t)\gamma(t)]$. Four different forms of the laws of the soliton adaptation to the external potentials Eqs. (102)–(105) tell the experimentalist how to compare various parameters in different application scenarios.

The exact integrability of the model [Eq. (98)] and novel soliton solutions provide novel experimental opportunities not only for the BEC physics but for the optical soliton physics as well. The parallels in nonlinear optics may be very fruitful. For example, let us consider the transformation of the variables

$$T=x;\ Z=-C_0^{-1}\ln(1-C_0t), \tag{107}$$

which establishes a one-to-one correspondence between the NLSE [Eq. (33)] with varying nonlinearity $R(t)=1/(1-C_0t)$ and the following NLSE with varying dispersion $D(Z)$,

$$i\frac{\partial\Psi}{\partial Z}+\frac{D(Z)}{2}\frac{\partial^2\Psi}{\partial T^2}+|\Psi|^2\Psi=0, \tag{108}$$

with the main difference being that dispersion is given by

$$D(Z)=\exp(-C_0Z). \tag{109}$$

Matter-wave solitons near the Feshbach resonance with periodically varying nonlinearity [Eqs. (49), (50)] are related to optical solitons through a rather complicated transformation of the variables,

$$T=x;\quad Z=\frac{2}{\omega\sqrt{1-\beta^2}}\tan^{-1}\left[\sqrt{\frac{1-\beta}{1+\beta}}\tan\left(\frac{\omega t}{2}\right)\right], \tag{110}$$

which establishes a one-to-one correspondence between the NLSE with periodically varying nonlinearity [Eqs. (49) and (50)] and the NLSE with periodically varying dispersion $D(Z)$,

$$i\frac{\partial\Psi}{\partial Z}+\frac{D(Z)}{2}\frac{\partial^2\Psi}{\partial T^2}+|\Psi|^2\Psi+\frac{x^2}{2}\frac{1}{D(Z)}\frac{\partial^2}{\partial t^2}\ln D(Z)\Psi=0, \tag{111}$$

where the dispersion management function is represented by

$$D(Z)=\frac{1+\beta}{\cos^2\left(\frac{1}{2}\omega Z\sqrt{1-\beta^2}\right)+\frac{1+\beta}{1-\beta}\sin^2\left(\frac{1}{2}\omega Z\sqrt{1-\beta^2}\right)}, \tag{112}$$

and Z is the propagation distance. Therefore, all effects considered in this article could be experimentally discovered

in nonlinear optics by using the dispersion-decreasing fibers with the core diameter changed along its length [50,51].

Our theory establishes an important interconnection between the varying-in-time nonlinearity and confining potential. A subtle interplay between nonlinear management by means of the Feshbach resonance on the one hand and linear management by means of confining time-dependent potential on the other hand can result in a rich variety of matter-wave solitons with several interesting properties. The experimental arrangement should be inspected to be as close as possible to the optimal map of parameters given by the laws of the soliton adaptation to the external potentials [see Eqs. (102)–(105)].

We conclude by saying that the concept of adaptation is of primary importance in nature, and nonautonomous solitons that interact elastically and generally move with varying amplitudes, speeds, and spectra adapted both to the external potentials and to the dispersion and nonlinearity changes can be fundamental objects of nonlinear science. The law of soliton adaptation to an external potential [20] has come as a surprise and this law is now the object of much concentrated attention in the field [52–67].

Nonlinear science is believed by many outstanding scientists to be the most deeply important frontier for understanding nature. The interpenetration of main ideas and methods being used in different fields of science and technology has become one of the decisive factors in the progress of science as a whole. Among the most spectacular examples of such an interchange of ideas and theoretical methods for analysis of various physical phenomena is the problem of solitary wave formation in the framework of the nonlinear Schrödinger equation models [Eqs. (97)–(100)] with linear and harmonic oscillator potentials. These models are used in a variety of fields of modern nonlinear science and probably will be able to play a basic role similar to that eventually played by the model of a quantum mechanical linear harmonic oscillator in the development of modern physics.

ACKNOWLEDGMENTS

The authors gratefully acknowledge useful conversations and illuminating discussions with Boris Malomed and Vladimir Konotop concerning the validity of the GPE model, its 3D-to-2D and 1D transformations and the problem of adiabaticity in nonlinear soliton management. We thank Svyatoslav Shlenov and Lubomir Kovachev for many helpful discussions about the operator splitting method based on 2D and 3D fast Fourier transform. Special thanks are due to our referee, who proposed the important studies of the validity of 1D nonautonomous soliton concept and, in particular, reversible 1D-to-3D transformations of BEC soliton due to its self-compression near the Feshbach resonance. This work has been supported by CONACYT and BUAP grants.

[1] E. A. Cornell and C. E. Wieman, Rev. Mod. Phys. **74**, 875 (2002); W. Ketterle, *ibid.* **74**, 1131 (2002).

[2] C. J. Pethick and H. Smith, *Bose-Einstein Condensation in Dilute Gases* (Cambridge University Press, Cambridge, UK, 2002).

[3] L. P. Pitaevskii and S. Stringari, *Bose-Einstein Condensation* (Oxford University Press, Oxford, US, 2003).

[4] P. G. Kevrekidis *et al.*, in *Emergent Nonlinear Phenomena in Bose-Einstein Condensates: Theory and Experiment*, edited by P. G. Kevrekidis, D. J. Frantzeskakis, and R. Carretero-González (Springer, Berlin, 2008).

[5] S. Burger, K. Bongs, S. Dettmer, W. Ertmer, K. Sengstock, A. Sanpera, G. V. Shlyapnikov, and M. Lewenstein, Phys. Rev. Lett. **83**, 5198 (1999); K. Bongs, S. Burger, D. Hellweg, M. Kottke, S. Dettmer, T. Rinkleff, L. Cacciapuoti, J. Arlt, K. Sengstock, and W. Ertmer, J. Opt. B **5**, 124 (2003).

[6] J. Denschlag, J. E. Simsarian, D. L. Feder, C. W. Clark, L. A. Collins, J. Cubizolles, L. Deng, E. W. Hagley, K. Helmerson, W. P. Reinhardt, S. L. Rolston, B. I. Scneider, and W. D. Phillips, Science **287**, 97 (2000).

[7] B. P. Anderson, P. C. Haljan, C. A. Regal, D. L. Feder, L. A. Collins, C. W. Clark, and E. A. Cornell, Phys. Rev. Lett. **86**, 2926 (2001).

[8] K. E. Strecker, G. B. Partridge, A. G. Truscott, and R. G. Hulet, Nature (London) **417**, 150 (2002); New J. Phys. **5**, 73 (2003).

[9] L. Khaykovich, F. Schreck, G. Ferrari, T. Bourdel, J. Cubizolles, L. D. Carr, Y. Castin, and C. Salomon, Science **296**, 1290 (2002).

[10] C. Becker, S. Stellmer, P. Soltan-Panahi, S. Dörscher, M. Baurmert, E.-M. Richter, J. Kronjäger, K. Bongs, and K. Sengstock, Nat. Phys. **4**, 496 (2008); S. Stellmer, C. Becker, P. Soltan-Panahi, E. M. Richter, S. Dorscher, M. Baumert, J. Kronjager, K. Bongs, and K. Sengstock, Phys. Rev. Lett. **101**, 120406 (2008).

[11] A. Weller, J. P. Ronzheimer, C. Gross, J. Esteve, M. K. Oberthaler, D. J. Frantzeskakis, G. Theocharis, and P. G. Kevrekidis, Phys. Rev. Lett. **101**, 130401 (2008).

[12] N. J. Zabusky and M. D. Kruskal, Phys. Rev. Lett. **15**, 240 (1965); N. J. Zabusky, Chaos **15**, 015102 (2005).

[13] P. L. Christiansen, M. P. Sorensen, and A. C. Scott, *Nonlinear Science at the Dawn of the 21st Century* (Springer, Berlin, 2000).

[14] A. Hasegawa, *Massive WDM and TDM Soliton Transmission Systems* (Kluwer Academic Publishers, Dordrecht/Norwell, MA, 2000).

[15] F. D. Tappert and N. J. Zabusky, Phys. Rev. Lett. **27**, 1774 (1971).

[16] H. H. Chen and C. S. Liu, Phys. Rev. Lett. **37**, 693 (1976); Phys. Fluids **21**, 377 (1978).

[17] C. S. Gardner, J. M. Greene, M. D. Kruskal, and R. M. Miura, Phys. Rev. Lett. **19**, 1095 (1967).

[18] F. Calogero and A. Degasperis, Lett. Nuovo Cimento **16**, 425 (1976); **16**, 434 (1976); F. Calogero and A. Degasperis, *Spectral Transform and Solitons: Tools to Solve and Investigate Nonlinear Evolution Equations* (North–Holland, Amsterdam/New York/Oxford, 1982).

[19] V. N. Serkin and A. Hasegawa, Phys. Rev. Lett. **85**, 4502 (2000); JETP Lett. **72**, 89 (2000); IEEE J. Sel. Top. Quantum Electron. **8**, 418 (2002); V. N. Serkin and T. L. Belyaeva, JETP Lett. **74**, 573 (2001); V. N. Serkin, A. Hasegawa, and T. L. Belyaeva, Phys. Rev. Lett. **92**, 199401 (2004).

[20] V. N. Serkin, A. Hasegawa, and T. L. Belyaeva, Phys. Rev. Lett. **98**, 074102 (2007).

[21] E. P. Gross, Nuovo Cimento **20**, 454 (1961); J. Math. Phys. **4**, 195 (1963); L. P. Pitaevskii, Zh. Eksp. Teor. Fiz. **40**, 646 (1961) [Sov. Phys. JETP **13**, 451 (1961)].

[22] A. N. Oraevsky, Quantum Electron. **31**, 1038 (2001).

[23] A. Hasegawa, *Optical Solitons in Fibers* (Springer-Verlag, Berlin, 1989);A. Hasegawa and Y. Kodama, *Solitons in Optical Communications* (Clarendon Press, New York, 1995); A. Hasegawa and M. Matsumoto, *Optical Solitons in Fibers* (Springer-Verlag, Berlin, 2003), 3rd ed.

[24] E. M. Dianov, P. V. Mamyshev, A. M. Prokhorov, and V. N. Serkin, *Nonlinear Effects in Fibers* (Harwood Academic, New York, 1989).

[25] J. R. Taylor, *Optical Solitons—Theory and Experiment* (University Press, Cambridge, UK, 1992).

[26] G. P. Agrawal, *Nonlinear Fiber Optics* (Academic Press, San Diego, 2001), 3rd ed.; G. P. Agrawal, *Applications of Nonlinear Fiber-Optics* (Academic Press, San Diego, 2001).

[27] N. N. Akhmediev and A. Ankiewicz, *Solitons. Nonlinear Pulses and Beams* (Charman and Hall, London, 1997).

[28] V. V. Konotop and L. Vazquez, *Nonlinear Random Waves* (World Scientific, Singapure, 1994).

[29] B. A. Malomed, *Soliton Management in Periodic Systems* (Springer, Berlin, 2006).

[30] A. J. Moerdijk, B. J. Verhaar, and A. Axelsson, Phys. Rev. A **51**, 4852 (1995).

[31] R. A. Duine and H. T. C. Stoof, Phys. Rep. **396**, 115 (2004).

[32] S. Inouye, M. R. Andrews, J. Stenger, H.-J. Meisner, D. M. Stamper-Kurn, and W. Ketterle, Nature (London), **392**, 151 (1998).

[33] Ph. Courteille, R. S. Freeland, D. J. Heinzen, F. A. van Abeelen, and B. J. Verhaar, Phys. Rev. Lett. **81**, 69 (1998).

[34] S. L. Cornish, N. R. Claussen, J. L. Roberts, E. A. Cornell, and C. E. Wieman, Phys. Rev. Lett. **85**, 1795 (2000).

[35] A. Görlitz, J. M. Vogels, A. E. Leanhardt, C. Raman, T. L. Gustavson, J. R. Abo-Shaeer, A. P. Chikkatur, S. Gupta, S. Inouye, T. Rosenband, and W. Ketterle, Phys. Rev. Lett. **87**, 130402 (2001); F. Schreck, L. Khaykovich, K. L. Corwin, G. Ferrari, T. Bourdel, J. Cubizolles, and C. Salomon, *ibid.* **87**, 080403 (2001).

[36] T. Weber, J. Herbig, M. Mark, H. C. Nägerl, and R. Grimm, Science **299**, 232 (2003); C. Chin, V. Vuletic, A. J. Kerman, S. Chu, E. Tiesinga, P. J. Leo, and C. J. Williams, Phys. Rev. A **70**, 032701 (2004); C. Chin, T. Kraemer, M. Mark, J. Herbig, P. Waldburger, H.-C. Nagerl, and R. Grimm, Phys. Rev. Lett. **94**, 123201 (2005).

[37] P. D. Lax, Commun. Pure Appl. Math. **21**, 467 (1968).

[38] M. J. Ablowitz, D. J. Kaup, A. C. Newell, and H. Segur, Phys. Rev. Lett. **31**, 125 (1973).

[39] V. E. Zakharov, in *Solitons*, edited by R. K. Bullough and P. J. Caudrey (Springer-Verlag, Berlin, 1980).

[40] M. R. Gupta and J. Ray, J. Math. Phys. **22**, 2180 (1981); J. J. E. Herrera, J. Phys. A **17**, 95 (1984); R. Balakrishnan, Phys. Rev. A **32**, 1144 (1985).

[41] J. E. Simsarian, J. Denschlag, M. Edwards, C. W. Clark, L. Deng, E. W. Hagley, K. Helmerson, S. L. Rolston, and W. D. Phillips, Phys. Rev. Lett. **85**, 2040 (2000); K. Bongs, S. Burger, S. Dettmer, D. Hellweg, J. Arlt, W. Ertmer, and K. Sengstock, Phys. Rev. A **63**, 031602(R) (2001); Yu. Kagan, E. L. Surkov, and G. V. Shlyapnikov, *ibid.* **54**, 1753(R) (1996); Y. Castin and R. Dum, Phys. Rev. Lett. **77**, 5315 (1996).

[42] H. H. Chen, Phys. Rev. Lett. **33**, 925 (1974).

[43] J. Satsuma and N. Yajima, Progr. Theor. Phys. Suppl. **55**, 284 (1974).

[44] H. Saito and M. Ueda, Phys. Rev. A **65**, 033624 (2002); L. Santos and G. V. Shlyapnikov, *ibid.* **66**, 011602(R) (2002); C. M. Savage, N. P. Robins, and J. J. hope, *ibid.* **67**, 014304 (2003).

[45] Y. B. Band and M. Trippenbach, Phys. Rev. A **65**, 053602 (2002); Y. B. Band, B. Malomed, and M. Trippenbach, *ibid.* **65**, 033607 (2002).

[46] K. Staliunas, S. Longhi, and G. J. de Valcarcel, Phys. Rev. Lett. **89**, 210406 (2002).

[47] J. A. Fleck, J. R. Morris, and M. D. Feit, Appl. Phys. **10**, 129 (1976); M. D. Feit and J. A. Fleck, Appl. Opt. **17**, 3990 (1978); J. S. Perkins and R. N. Baer, J. Acoust. Soc. Am. **72**, 515 (1982); G. J. Orris and J. S. Perkins, *ibid.* **103**, 3029 (1998); O. V. Sinkin, R. holzlohner, J. Sweck, and C. R. Menyuk, J. Lightwave Technol. **21**, 61 (2003); S. A. Shlenov, Ph.D. thesis, Moscow State University, 1986; S. S. Chesnokov, V. P. Kandidov, S. A. Shlenov, and M. P. Tamarov, in *Proceedings of SPIE The International Society for Optical Engineering*, Vol. 3432, p. 14 (1998); L. M. Kovachev, Opt. Express **15**, 10318 (2007); J. Mod. Opt. **55**, 2975 (2008); **56**, 1797 (2009); AIP Conf. Proc. **1186**, 69 (2009).

[48] V. V. Afanas'ev, E. M. Dianov, A. M. Prokhorov, and V. N. Serkin, Pis'ma v Zh. Eksp. Teor. Fiz. **48**, 588 (1988) [JETP Lett. **48**, 638 (1988)]; V. V. Afanasjev, E. M. Dianov, and V. N. Serkin, IEEE J. Quantum Electron. **25**, 2656 (1989); V. V. Afanasyev, Y. S. Kivshar, V. V. Konotop, and V. N. Serkin, Opt. Lett. **14**, 805 (1989); T. Kohler and K. Burnett, Phys. Rev. A **65**, 033601 (2002).

[49] S. J. Wang, C. L. Jia, D. Zhao, H. G. Luo, and J. H. An, Phys. Rev. A **68**, 015601 (2003).

[50] S. A. Ponomarenko and G. P. Agrawal, Phys. Rev. Lett. **97**, 013901 (2006); Opt. Lett. **32**, 1659 (2007); Opt. Express **15**, 2963 (2007).

[51] P. C. Reeves-Hall and J. R. Taylor, Electron. Lett. **37**, 417 (2001); P. C. Reeves-Hall, S. A. E. Lewis, S. V. Chernikov, and J. R. Taylor, *ibid.* **36**, 622 (2000); J. C. Travers, J. M. Stone, A. B. Rulkov, B. A. Cumberland, A. K. George, S. V. Popov, J. C. Knight, and J. R. Taylor, Opt. Express **15**, 13203 (2007).

[52] V. N. Serkin and T. L. Belyaeva, Quant. Electron. **31**, 1007 (2001); T. C. Hernandez *et al.*, *ibid.* **35**, 778 (2005); C. H. Tenorio *et al.*, *ibid.* **35**, 929 (2005); C. Hernandez-Tenorio, T. L. Belyaeva, and V. N. Serkin, Physica B **398**, 460 (2007).

[53] R. Atre, P. K. Panigrahi, and G. S. Agarwal, Phys. Rev. E **73**, 056611 (2006).

[54] S. Chen, Y. H. Yang, L. Yi, P. Lu, and D. S. Guo, Phys. Rev. E **75**, 036617 (2007).

[55] K. Porsezian, R. Ganapathy, A. Hasegawa, and V. N. Serkin, IEEE J. Quantum Electron. **45**, 1577 (2009); R. Ganapathy, K. Porsezian, A. Hasegawa, and V. N. Serkin, *ibid.* **44**, 383 (2008); K. Porsezian, A. Hasegawa, V. N. Serkin, T. L. Belyaeva, and R. Ganapathy, Phys. Lett. **A361**, 504 (2007).

[56] L. Wu, J. F. Zhang, L. Li, C. Finot, and K. Porsezian, Phys. Rev. A **78**, 053807 (2008); J. F. Zhang, L. Wu, and L. Li, *ibid.* **78**, 055801 (2008).

[57] M. Belic, N. Petrovic, W. P. Zhong, R. H. Xie, and G. Chen, Phys. Rev. Lett. **101**, 123904 (2008).

[58] R. Hao and G. Zhou, Opt. Commun. **281**, 4474 (2008); J. Wang, L. Li, and S. Jia, J. Opt. Soc. Am. B **25**, 1254 (2008); Q. Y. Li, Z. D. Li, S. X. Wang, W. W. Song, and G. Fu, Opt. Commun. **282**, 1676 (2009).

[59] L. Wu, L. Li, G. Chen, Q. Tian, and J. F. Zhang, New J. Phys. **10**, 023021 (2008); L. Wu, L. Li, J. F. Zhang, Phys. Rev. A **78**, 013838 (2008).

[60] H. J. Shin, J. Phys. A **41**, 285201 (2008).

[61] T. Xu, C. Y. Zhang, G. M. Wei, J. Li, X. H. Meng, and B. Tian, Eur. Phys. J. B **55**, 323 (2007); W. J. Liu, B. Tian, and H. Q. Zhang, Phys. Rev. E **78**, 066613 (2008).

[62] D. Zhao, X. G. He, and H. G. Luo, Eur. Phys. J. D **53**, 213 (2009); D. Zhao, H. G. Luo, and H. Y. Chai, Phys. Lett. **A372**, 5644 (2008).

[63] A. T. Avelar, D. Bazeia, and W. B. Cardoso, Phys. Rev. E **79**, 025602(R) (2009).

[64] L. Li, X. Zhao, and Z. Xu, Phys. Rev. A **78**, 063833 (2008); X. Zhao, L. Li, and Z. Xu, *ibid.* **79**, 043827 (2009).

[65] H. G. Luo, D. Zhao, and X. G. He, Phys. Rev. A **79**, 063802 (2009); X. G. He, D. Zhao, L. Li, and H. G. Luo, Phys. Rev. E **79**, 056610 (2009).

[66] F. Wang, X. Yan, D. Wang, and J. Ding, Mod. Phys. Lett. B **23**, 2311 (2009).

[67] Z. Yan and V. V. Konotop, Phys. Rev. E **80**, 036607 (2009).